Can Azomethine Ylides be Considered as Frustrated Lewis Pairs?

Sudip Baguli,[a] Subham Sarkar,[a,b] Dibyendu Mallick,*[b] Debabrata Mukherjee*[a]

[a] Department of Chemical Sciences, Indian Institute of Science Education and Research Kolkata, Mohanpur, Nadia, 741246, India.

[b] Department of Chemistry, Presidency University, 86/1 College Street, Kolkata, 700073, India.

Azomethine Ylide • Frustrated Lewis Pair • Small Molecule Activation • Reaction mechanism • Density Functional Theory calculations.

ABSTRACT: Azomethine ylides are typically transient synthons, heavily used in constructing N-heterocycles by dipolar cycloaddition reactions. We report here a pyridyl-tethered isolable azomethine ylide (**AY**) that unprecedentedly acts as a Frustrated Lewis Pair (FLP) in activating a series of H–E bonds (E = B, Si, Al, O). The reactions are thoroughly probed mechanistically by the aid of DFT calculations and each case appears to be distinct from the rest. While the HBpin activation follows a stepwise mechanism, the same of $PhSiH_3$ has a concerted route. The AlH_3 activation is also stepwise but takes place across the 1,5-(C^+/N^-) dipole involving the pyridyl-*N*. The H_2O activation is better fitted with a 'relay' mechanism with two H_2O molecules rather than one to interact with **AY**. The B–B bond of B_2pin_2 is also cleaved but in an intriguingly different way, by an oxidative addition at a carbene center formed in situ through a 1,3-(C^+ to C^-) H^+ shift. Though the imperative H_2 activation fails, a transfer hydrogenation by NH_3•BH_3 is achieved readily and mechanistically elucidated as a stepwise process. The **AY** also undergoes FLP-like cycloadditions with various dipolarophiles, among which the addition of CS_2 but not of CO_2 is alluring and counter-intuitive. DFT analysis again justifies this dichotomy by showing the addition of CS_2 as thermodynamically favored but of CO_2 as disfavored, mostly due to the larger ring strain in the cycloaddition product in the CO_2 case.

Introduction

Stephan's report on the metal-free and reversible activation of H_2 in 2006[1] by a so called "*frustrated Lewis pair*" (FLP) has truly revolutionized the chemistry of main group elements, particularly in the quest for drawing transition metal-like behavior from them.[2] As the name suggests, a FLP consists of a Lewis acid and a Lewis base, intra- or intermolecularly, that are sterically denied from a bonding interaction between them (Figure 1). Due to this restraint, their unsatisfied Lewis characters can synergistically split or trap a new molecule. This innovative strategy has been a hot topic for the p-block in activating and catalytically sequestering strong bonds and small molecules, which is otherwise challenging and typically the forte of transition metals.[3] Such processes are also well-inspected mechanistically, especially by DFT calculation.[4] Interestingly, seemingly robust Lewis adducts can also exhibit FLP-like nature, likely by transiently disengaging their acidic and basic sites.[5]

Among the metal-free FLPs, the major choices are boron and phosphorus-centered acids and bases, respectively, while other donors (N, C, O, S) and acceptors (C, Si, $P^{(V)}$) have also emerged in expanding and tuning this new chemistry frontier.[6] In this regard, ambiphilic and valence-unsaturated carbenes, especially Bertrand's (alkyl)(amino)carbenes, are intriguing cases of purely C-centered FLPs, where singlet carbene centers act as both the Lewis acidic and basic sites (Figure 1).[7] They are also able to activate a series of strong bonds and small molecules including the difficult H_2, but in mostly stoichiometric fashion.[8]

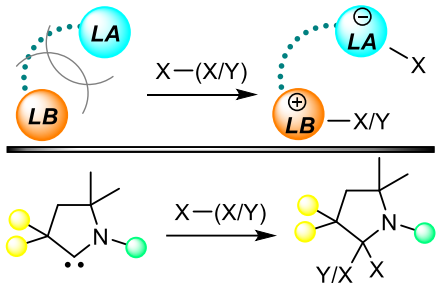

Figure 1. Schematic diagrams of a FLP (***top***) and a cyclic(alkyl)(amino)carbene (***bottom***) and bond activations by them.

On a separate note, we have recently shown that a barrelene-derived azomethine ylide (**AY**) with a pyridyl arm isomerizes to a cyclic(amino)(barrelene)carbene by a 1,3-H^+ shift at 60 °C driven by a CuCl (Figure 2).[9] Without CuCl, **AY** isomerizes to its aziridine form at 80 °C (Figure 2).[9] Conceptually, the 1,3-dipolar **AY** can be considered as another purely C-centered FLP while the aziridine as its 'satisfied' version. One can also imagine **AY** as an '*outstretched carbene'*, where the single site ambiphilicity is decoupled over two different carbons separated by an iminium-*N*. In fact, the cycloadditions of azomethine ylides with dipolarophiles, the prime uses of these synthons,[10] can be viewed as FLPs (the azomethine ylides) activating small molecules (dipolarophiles). Notably, azomethine ylides are mostly

transient in nature, often generated in situ under the cycloaddition reaction conditions. Their isolated variants like the present case are rare and stabilized by delocalizing the charges.[11]

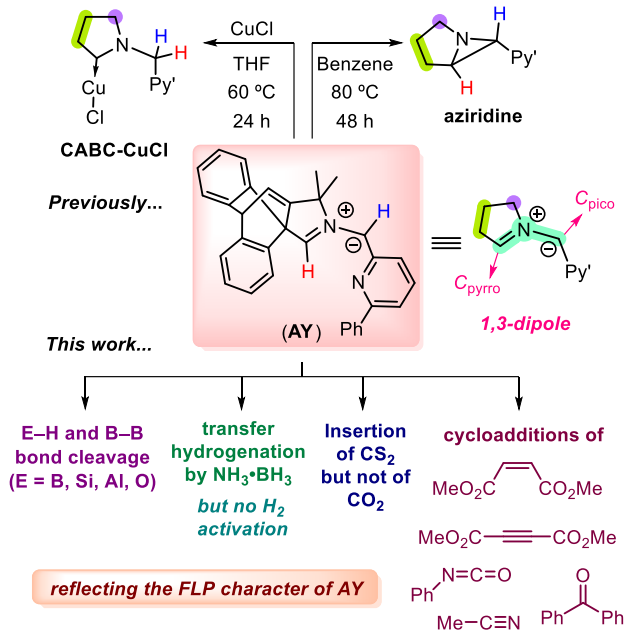

Figure 2. (***top***): An azomethine ylide (**AY**) and its isomerization into an aziridine and a carbene-CuCl complex;[9] (***bottom***): the FLP nature of **AY** (*this work*).

Given the decent kinetic stability of **AY** and sensing a potential FLP relation, we report here its truly FLP-styled activations of E–H (E = B, Al, Si, O) and B–B bonds, unprecedented for this organic class. In addition, though the difficult H_2 activation fails, **AY** is a transfer hydrogenated by NH_3•BH_3 under a mild condition. The activation mechanisms are probed by DFT analysis, where each reaction proves to follow a distinct route than the rest. Furthermore, **AY** distinguishes between CO_2 and CS_2 counter-intuitively by staying inert to the former but easily cycloadding the latter, which is again validated by DFT analysis. Of note, FLPs are well explored in trapping and functionalizing the greenhouse gas CO_2.[12] CS_2 is also an environmental pollutant as well as synthetically important, but a similar FLP treatment is less explored[13] and trapping by an azomethine ylide is unprecedented to the best of our knowledge. Lastly, **AY** also undergoes typical 1,3-dipolar cycloadditions with a bunch of other dipolarophiles.

Results and Discussion

E-H (E = B, Si, Al, O) and B-B bond activations

AY readily cleavages the H–B bond of HBpin to give **1** at room temperature (Scheme 1) as a colorless solid, confirmed by X-ray crystallography (Figure 3) and supported by NMR chemical shifts. The three-coordinate boron is evident from its ^{11}B chemical shift at 20.1 ppm. DFT calculations show the frontier molecular orbitals of **AY** spread over its 1,3-dipole with the HOMO-LUMO energy gap of 3.3 eV (Figure S74). The Fukui function analysis (see SI) marks C_{pico} as the most nucleophilic site. DFT analyses suggest not a concerted but a stepwise route for this H–B bond cleavage, where the C_{pico} first makes a bond with the Lewis acidic boron of HBpin to give a zwitterionic intermediate (**Int**) that delivers the hydride onto the C_{pyrro} (Figure 4). The *H* transfer step is the rate determining step with an energy barrier of 20.5 kcal/mol, while **1** gets a net stability of 19.3 kcal/mol. To check if the pyridyl moiety is critical, a modified pyrrolinium salt **[2]Br** is made by replacing the pyridyl with an aryl group. Its following deprotonation gives a new azomethine ylide **3**, but that is far less stable than **AY** and is converted to the aziridine **4** at room temperature within 6 h (Scheme 1). Yet, an in situ formed **3** reacts readily with HBpin also by a similar H–B bond activation to give **5** as evident from NMR spectroscopy and high-resolution mass spectrometry. Hence, the HBpin activation looks possible even without the pyridyl sidearm. This is also validated by computation that shows no potential interaction between **AY**-N_{py} and the Bpin moiety at any point of the reaction. A stable Lewis pair $B(C_6F_5)_3$/DABCO cleaves HBpin to give $[(DABCO)Bpin]^+[HB(C_6F_5)_3]^-$.[14] **AY** with non-hydridic and stronger Lewis acidic boranes like BF_3 and $B(C_6F_5)_3$ give stable zwitterionic borates **6** and **7** (Scheme 1) that resemble the proposed **Int** in the HBpin case. Borane adducts of carbenes and a phosphorus ylide are known.[15] An attempt to deprotonate **6** and **7** by KHMDS gives no isolable product in either case.

The H–Si bond cleavage of $PhSiH_3$ is also accomplished at room temperature to give **8** (Scheme 1) as a light-yellow oil. But the reaction is slower than HBpin activation and takes nearly 10 h to complete. Though the oily nature forbids an X-ray characterization of **8**, its NMR spectroscopic data agree well with the given bond connectivity. The two diastereotopic -SiH_2 protons appear as two doublets of doublets at 5.24 ($^2J_{HH}$ = 6.8 Hz and $^3J_{HH}$ = 2.4 Hz) and 5.08 ($^2J_{HH}$ = 6.8 Hz and $^3J_{HH}$ = 2.8 Hz) ppm, respectively. The corresponding ^{29}Si resonance appears at –31.7 ppm ($^1J_{Si\text{-}H}$ = 173 Hz). Interestingly, unlike the HBpin case, DFT analysis suggests a concerted route for the H–Si bond activation to give **8** (Figure 4). The difference likely arises from the more prominent Lewis acidic nature of HBpin than $PhSiH_3$ due to the availability of an empty 2p orbital on boron that can readily interact with C_{pico}. In the case of $PhSiH_3$, the NBO analysis (Table S4 and S5) of the TS_{HSi} shows a simultaneous involvement of the σ and σ* of the H–Si bond. The corresponding energy barrier (24.4 kcal/mol) is roughly 4 kcal/mol higher than the *H* transfer (20.5 kcal/mol) in the HBpin case, which justifies the relatively sluggish activation of the H–Si bond. Cyclic(alkyl)(amino)carbenes (CAACs) cleave the same H–B and H–Si bonds within similar timelines as shown by **AY**.[8c, 16] Notably, $(Mes)_2PCH_2CH_2B(C_6F_5)_2$ (Mes = 2,4,6-Me_3-C_6H_2), an intramolecular FLP, activates $PhSiH_3$ reversibly.[17]

Scheme 1. Reactivity of AY towards HBpin, BX_3 (X = F, C_6F_5), $PhSiH_3$, $AlH_3(NMe_2Et)$, H_2O, $PhCH_2OH$, MeI, B_2pin_2, H_2, and BH_3•NH_3. Individual reactions are differently color-coded.

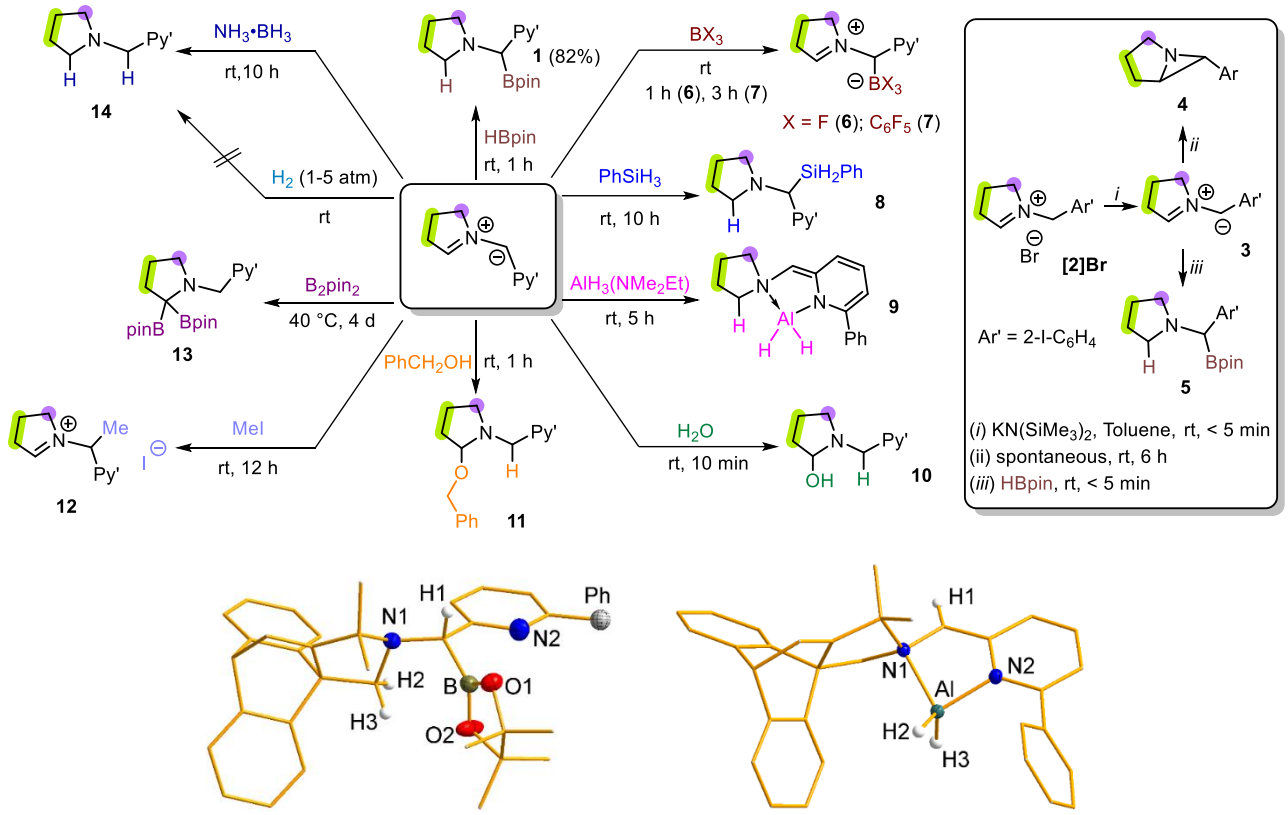

Figure 3. DIAMOND-rendered molecular structures of **1** (***left***) and **9** (***right***). Relevant ellipsoids are drawn at 50% probability level. The rest of the skeletons are depicted by wires. Only the relevant hydrogen atoms are shown. The phenyl ring on the pyridyl moiety is slightly disordered in **1** and is not shown explicitly. Selected bond lengths (Å): **9**: N1-Al 2.0206(11), N2-Al 1.8899(12).

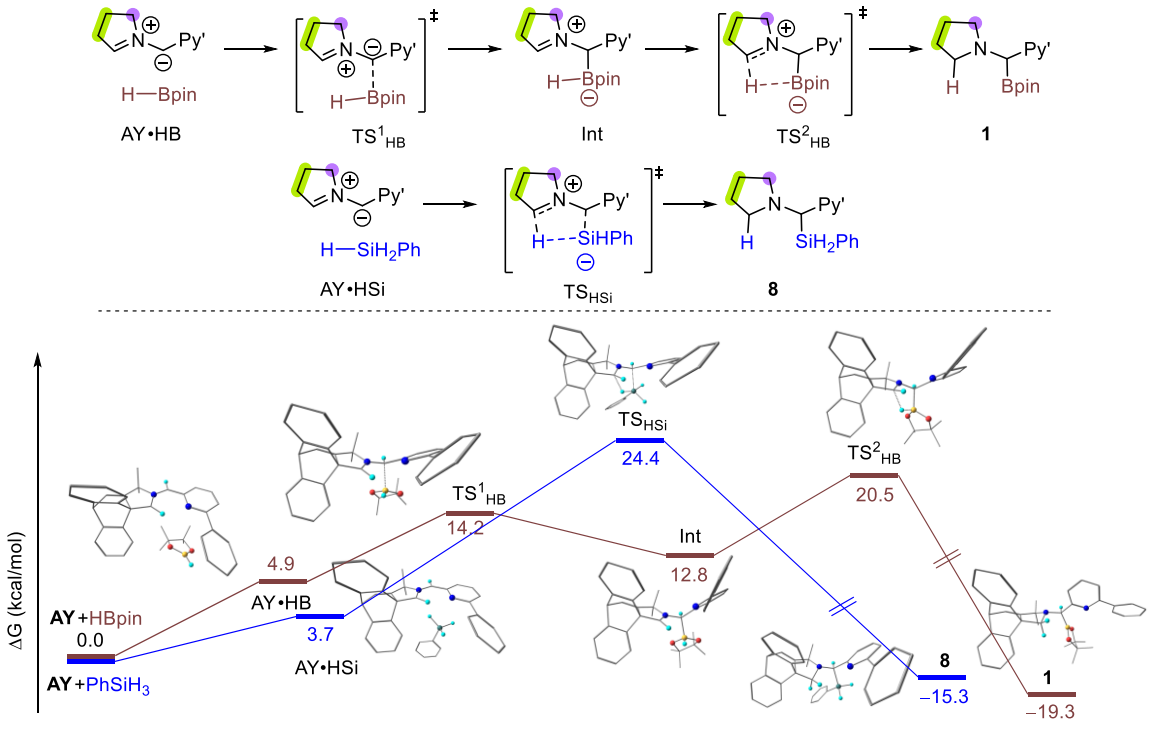

Figure 4. DFT-proposed mechanisms for HBpin and $PhSiH_3$ activations by **AY** (***top***) and the corresponding energy profile diagrams calculated at B3LYP-D3(BJ)/B2//B3LYP-D3(BJ)/B1 level of theory using benzene as an implicit solvent (SMD model) (***bottom***).

Interestingly, unlike the H–E (E = B, Si) bond activations, **AY** uses its 1,5-dipole instead of 1,3- to cleave the more polar H–Al bond of AlH_3, giving **9** (Scheme 1) as a dark red solid as shown by X-ray crystallography (Figure 3). Apart from the two terminal hydrides, the four-coordinate tetrahedral Al is also bound to the pyrrolidine-*N* to produce a five-membered

metallacycle. The dearomatized picolyl moiety is clearly evident in the ^{1}H NMR spectrum.[18] The DFT-suggested mechanism (Figure 5) shows the dearomatized picolyl-*N* to bind the AlH_3 first to give an aluminate intermediate [AY•AlH_3] that self-adjusts by bond rotations to go to a higher energy form [AY•AlH_3]' before transferring the Al–*H* onto the C_{pyrro} to give **9**. The net barrier for the Al-*H* transfer is 15.1 kcal/mol, while the product **9** is 47.2 kcal/mol more stable than the starting combination of **AY** and AlH_3. A hypothetical H–Al activated product (**9'**) across the 1,3-dipole of **AY** is found to be 10.6 kcal/mol less stable than **9**. CAACs undergo 1,1-hydroalumination with AlH_3 at the carbene, which could be reversible as suggested by variable temperature NMR experiments.[19] Though aluminum is being heavily explored as a Lewis acidic site in the FLP context,[20] we are not aware of cleaving an alane molecule by a FLP in the manner noted here.

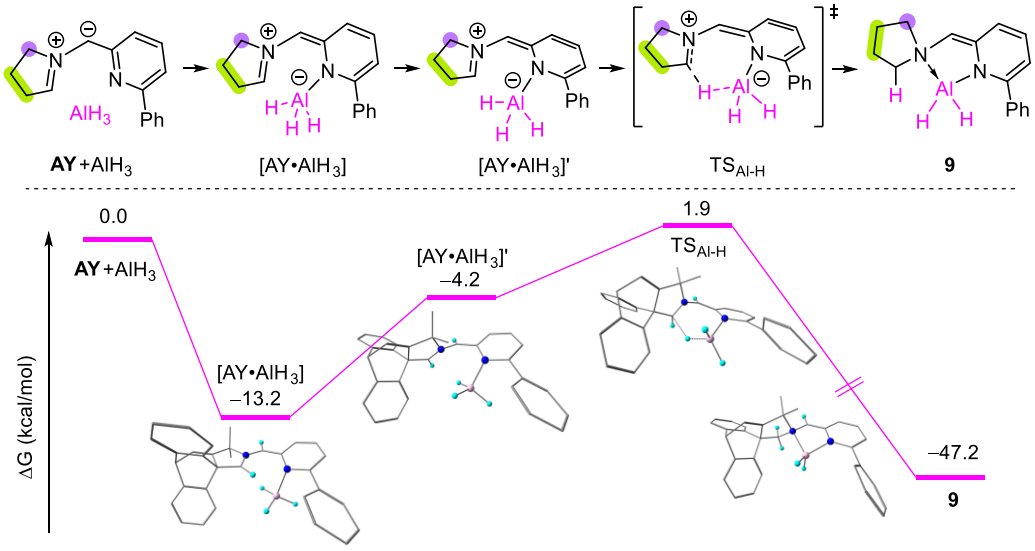

Figure 5. Proposed mechanism for alane activation by the 1,5-dipole of **AY** (***top***) and the corresponding energy profile diagram calculated at B3LYP-D3(BJ)/B2//B3LYP-D3(BJ)/B1 level of theory using benzene as an implicit solvent (SMD model) (***bottom***).

Metal-free FLPs are usually moisture-sensitive, binding a H_2O molecule or splitting it into H^+ and OH^- across its Lewis basic and acidic sites, respectively.[21] Despite the decent thermal stability, **AY** is moisture sensitive and rapidly splits a molecule of H_2O to give **10** (Scheme 1).[9] This seemingly straightforward hydrolysis shows an interesting mechanistic twist on probing by computation. Given the stoichiometry is 1:1, calculation considering one H_2O molecule suggests path ***A*** (Figure 6), where two tandem deprotonations would first give a picolyl-CAAC intermediate ($Int_{AY\text{-}1}$•H_2O) and a new H_2O molecule. The CAAC would then add that H_2O in an oxidative addition fashion to give **10**.[22] If this is true, **AY** and D_2O (1:1) should result into H/D scrambling in CAAC(*H*)(O*H*) of **10**. But it is experimentally not the case and thus route ***A*** can be ruled out. An alternative 'relay mechanism'[23] with two H_2O molecules gives a markedly different route ***B*** (Figure 6). There, protonating the C_{pico} by the water dimer gives a transient ion pair [pyrrolinium]$^+$[H_2O---HO]$^-$ ($Int_{AY\text{-}2}$) that goes on to give **10** by planting the OH^- to the C_{pyrro}. In that case, **AY** should split D_2O into D^+ on C_{pico} and OD^- on C_{pyrro} without scrambling the C_{pyrro}-*H*. It is indeed noticed experimentally. ***B*** is also an overall lower energy ($\Delta G^{‡}$ = 19.7 kcal mol^{-1}) pathway than ***A*** ($\Delta G^{‡}$ = 24.0 kcal mol^{-1}). $PhCH_2OH$ is similarly cleaved by its O–H bond to give the ether **11** (Scheme 1) as shown by NMR spectroscopy and verified by X-ray crystallography (Figure S71; SI). Activating a single molecule of H_2O by an intermolecular B/P-based FLP is computationally modelled.[21d] Another B/P-based intramolecular FLP cleaves a phenolic O–H reversibly.[24]

MeI adds the Me^+ to the C_{pico} of **AY** to give a new pyrrolinium salt **12** (Scheme 1), which again reflects C_{pico} as the most nucleophilic site. A subsequent deprotonation of **12** could potentially lead to a methylated-**AY**, but the reaction with KHMDS fails to yield any clean species.

AY also cleaves the homo-dinuclear B–B bond of B_2pin_2, but in an intriguingly different manner than the aforementioned cases to give **13** (Scheme 1) as a light-yellow powder. The reaction is also slower than even the H–Si bond activation, taking four days to complete at 40 °C. Surprisingly, some of the critical ^{1}H and ^{13}C{^{1}H} NMR chemical shifts in C_6D_6 at room temperature are broad, which makes it difficult to identify **13** that readily. But the spectra at –20 °C in tol-d_8 show sharp signals that suggest the depicted bond connectivity. The picolyl-CH_2 give two signature diastereotopic doublets ($^{2}J_{HH}$ = 15.0 Hz) at 5.30 and 4.60 ppm, respectively. Only a single broad signal at 21.9 ppm is noted in the ^{11}B NMR spectrum. Though it is yet to be structurally proved, **13**'s high-resolution mass spectrum at least verifies its composition. The mechanism seems to be alluring and needs more deliberation. A simplified schematic diagram is given in the SI (Figure S75). The 1,3-H^+ shift from C_{pyrro} to C_{pico} is evident, which could convert C_{pyrro} into a CAAC that can oxidatively add B_2pin_2 to give **13**. As noted in the CuCl-driven CAAC generation from **AY** by a similar 1,3-H^+ switch,[9] B_2pin_2 also likely plays a critical role here in steering that H^+ shift. Oxidative addition of B_2pin_2 at ^{Me2}CAAC is facile at room temperature.[8g]

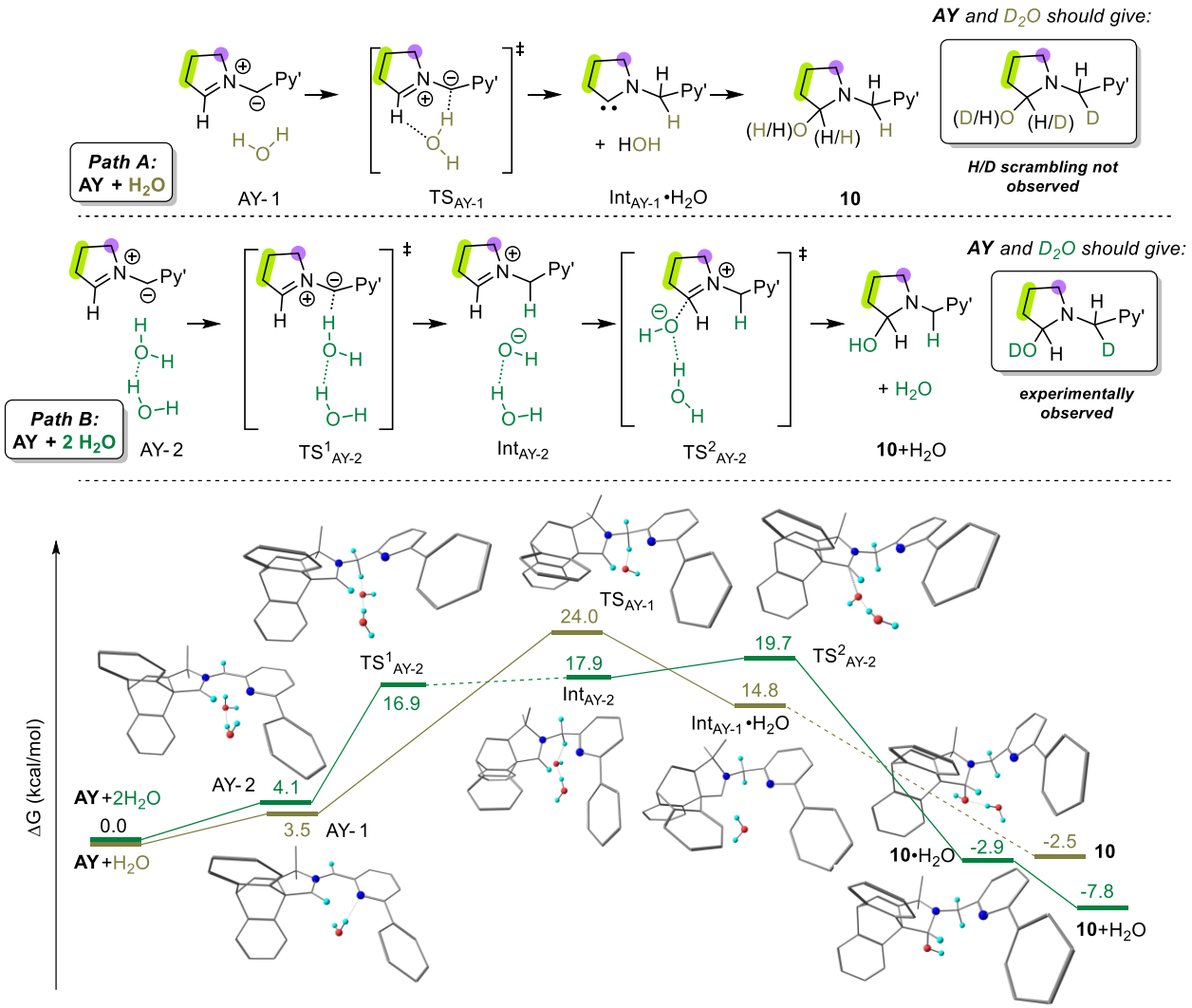

Figure 6. Computed hydrolysis routes of **AY** considering one and two molecules of H_2O, respectively (***top***) and the corresponding energy profile diagrams calculated at B3LYP-D3(BJ)/B2//B3LYP-D3(BJ)/B1 level of theory using benzene as an implicit solvent (SMD model) (***bottom***).

No H_2 activation but transfer hydrogenation by NH_3•BH_3

Unfortunately, **AY** fails to activate the imperative H_2 (p_{H2} = 1 bar) within 25-80 °C before it isomerizes into the aziridine.[9] DFT analysis on a hypothetical H–H bond cleavage across the 1,3-dipole of **AY** shows a concerted route similar to Si–H bond activation with an activation barrier of 29.7 kcal/mol (Figure 7). Though it seems not unachievable, poor solubility of H_2 may defer the process. The limited thermal stability of **AY** is also an issue since heating beyond 80 °C is not an option. Increasing the p_{H2} to 10 bar shows a complete conversion but only to an intractable mixture, from which the hydrogenated product is not identified. It should be noted that unlike the CAACs, the less ambiphilic imidazolidine-based NHCs (N-heterocyclic carbenes) are inert towards H_2.[8e]

The ammonia-borane adduct (NH_3•BH_3; **AB**) has emerged as a promising hydrogen storage material, acting as a convenient H_2 surrogate in transfer hydrogenation reactions.[25] FLPs including carbenes are known to dehydrogenate **AB**.[26] Some of them, but not the carbenes, can be catalytic. In this case, though the direct hydrogenation fails, **AY** is transfer hydrogenated by **AB** at room temperature to give the hydrogenated product **14** (Scheme 1) as a yellowish semi-solid. It is also characterized by X-ray diffraction (Figure 7). DFT analysis shows a stepwise route (Figure 7), adding a N–*H* first to the C_{pico} followed by a B-*H* transfer to the C_{pyrro}. Like in the HBpin case, here also the *H* transfer step has the highest energy barrier of 19.9 kcal/mol that is ~10 kcal/mol lower than the hypothetical H–H bond cleavage ($\Delta G^{\ddagger}$ = 29.7 kcal mol^{-1}). Furthermore, the transfer hydrogenation reaction with **AB** is more exergonic (ΔG = −30.7 kcal mol^{-1}) compared to the direct hydrogenation (ΔG = −21.8 kcal mol^{-1}). Thus, the lower kinetic barrier, higher product stability, and the far better solubility of **AB** than H_2 explain the facile nature of this transfer hydrogenation.

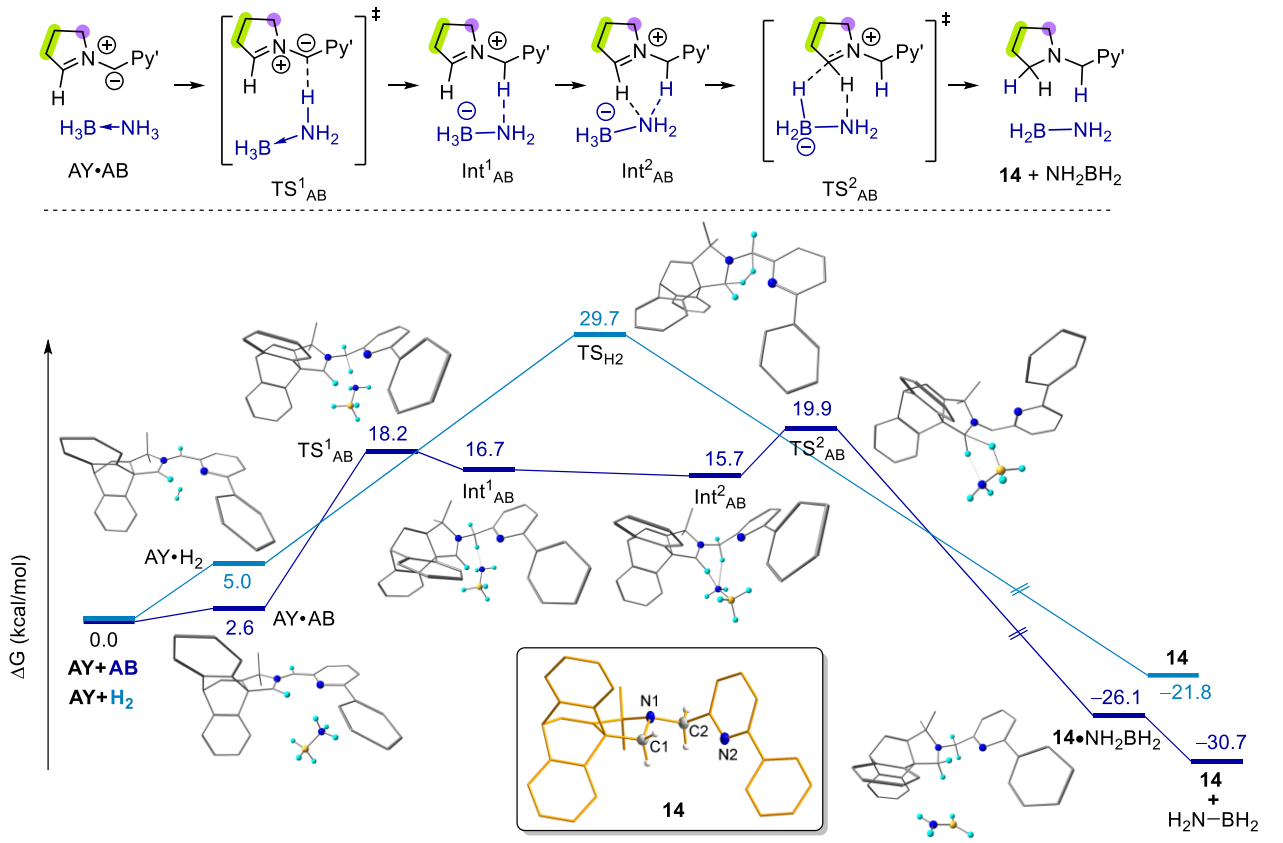

Figure 7. DFT-established mechanism (***top***) for the transfer hydrogenation of **AY** by NH_3•BH_3 and the corresponding energy profile diagram calculated at B3LYP-D3(BJ)/B2//B3LYP-D3(BJ)/B1 level of theory using benzene as an implicit solvent (SMD model) (***bottom***). Another computed energy profile for the hypothetical hydrogenation is also included in the same diagram. **Inset:** DIAMOND-rendered molecular structure of **14**. Relevant ellipsoids are drawn at 50% probability level. The rest of the skeleton is depicted by wires. Only the relevant hydrogen atoms are shown.

Reactivity with dipolarophiles including CX_2 (X = O, S)

Intriguingly, like in the H_2 case, **AY** stays inert towards CO_2 (1 atm) before isomerizing to the aziridine above 80 °C. But it swiftly reacts with CS_2 by [3+2]-cycloaddition to give **15** (Scheme 2) as seen by NMR spectroscopy. Curiously, **15** exists in its tautomeric form **15'** in the solid-state (Figure 8), where the C_{pico}–*H* proton migrates onto the pyridyl-*N* and interacts with the exocyclic S^-. The existence of **15'** is not noticed though in solution even at –80 °C as suggested by the ^{1}H NMR spectrum in toluene-d_8. Carbenes in comparison typically form zwitterionic adducts with both CO_2 and CS_2.[27]

Scheme 2. Reactivity of AY towards CX_2 (X = O, S), dimethyl maleate, dimethyl but-2-ynedioate, benzophenone, phenyl isocyanate, and acetonitrile.

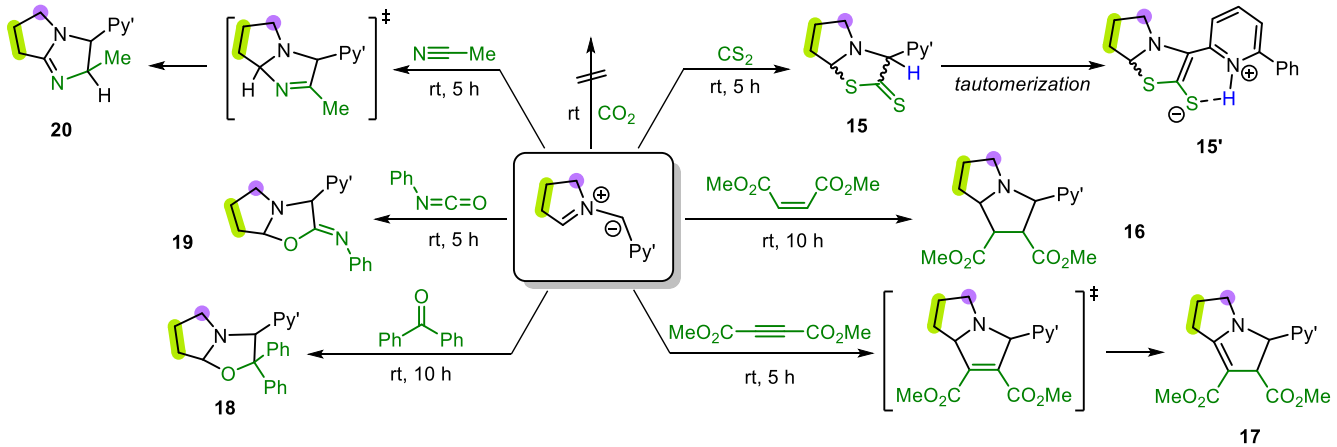

https://doi.org/10.26434/chemrxiv-2024-b2r6c **ORCID:** https://orcid.org/0000-0002-3678-0593

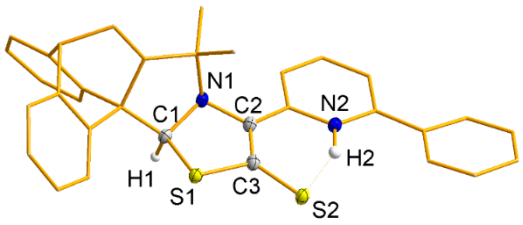

Figure 8. DIAMOND-rendered X-ray crystal structure of **15'**. Relevant ellipsoids are drawn at 50% probability level. The rest of the skeletons are depicted by wires. Only the relevant hydrogen atoms are shown. Selected bond lengths (Å): C1-S1 1.8810(16), C3-S1 1.7538(17), C3-S2 1.7052(18), C2-C3 1.3853(24), S2---H2 1.989(26).

Since CO_2 is more electrophilic than CS_2,[28] this dichotomic reactivity is counter-intuitive but can be justified by DFT analysis (Figure 9). Gas-phase calculations indicate that the reaction with CS_2 is favored thermodynamically by 5.8 kcal/mol but disfavored with CO_2 by 8.8 kcal/mol. This is rationalized by decomposing the reaction energies (ΔE_{tot}) of the cycloaddition products **15** and the hypothetical $\mathbf{15}_{CO2}$ by distortion and interaction energies; i.e. $\Delta E_{tot} = \Delta E_{dist} + \Delta E_{int}$.[29] Although bonding interactions stabilize the CO_2 adduct, the strain arising from distortion of the reactants while going from reactant to product would destabilize it. Calculations show that the ΔE_{int} for CO_2 (–162.6 kcal/mol) is expectedly higher than that for CS_2 (–129.3 kcal/mol). But the ring strain, as evident from the changes in bond angles and lengths on going from the isolated reactants to the product (Table 1), is more severe at the same time for CO_2 (ΔE_{dist} = 157.2 kcal/mol) than for CS_2 (ΔE_{dist} = 109.0 kcal/mol). Hence, the net electronic energy gain for the cycloaddition of CO_2 is −5.4 kcal mol^{-1}, which is much less than that of CS_2 (–20.3 kcal mol^{-1}). We further note that the electronic stabilization gained by the cycloaddition of CO_2 is insufficient to overcome the entropic penalty, which essentially disfavors the reaction thermodynamically. Whereas CS_2's entropic penalty is well compensated by the sufficient electronic stability of its product **15**. Furthermore, the tautomeric **15'** has an additional thermodynamic stability of 1.5 kcal/mol compared to **15**, that supports the former's dominance in the solid state. A hypothetically tautomerized $\mathbf{15'}_{CO2}$ in contrast is destabilized by 3.2 kcal/mol from $\mathbf{15}_{CO2}$ for the same strain factor. Calculations also show the CS_2 insertion from above and below the **AY**'s 1,3-dipole has similar activation barriers (Figure S76). Thus, the two chiral centers in **15** should not be stereoselective and the tautomeric **15'** should exist as a racemic mixture upon annulling C_{pico}'s chirality. Indeed, the unit cell of **15'** has both the enantiomers present. The lack of stereoselectivity at the C_{pico} in all the above bond activation cases are also evident experimentally.

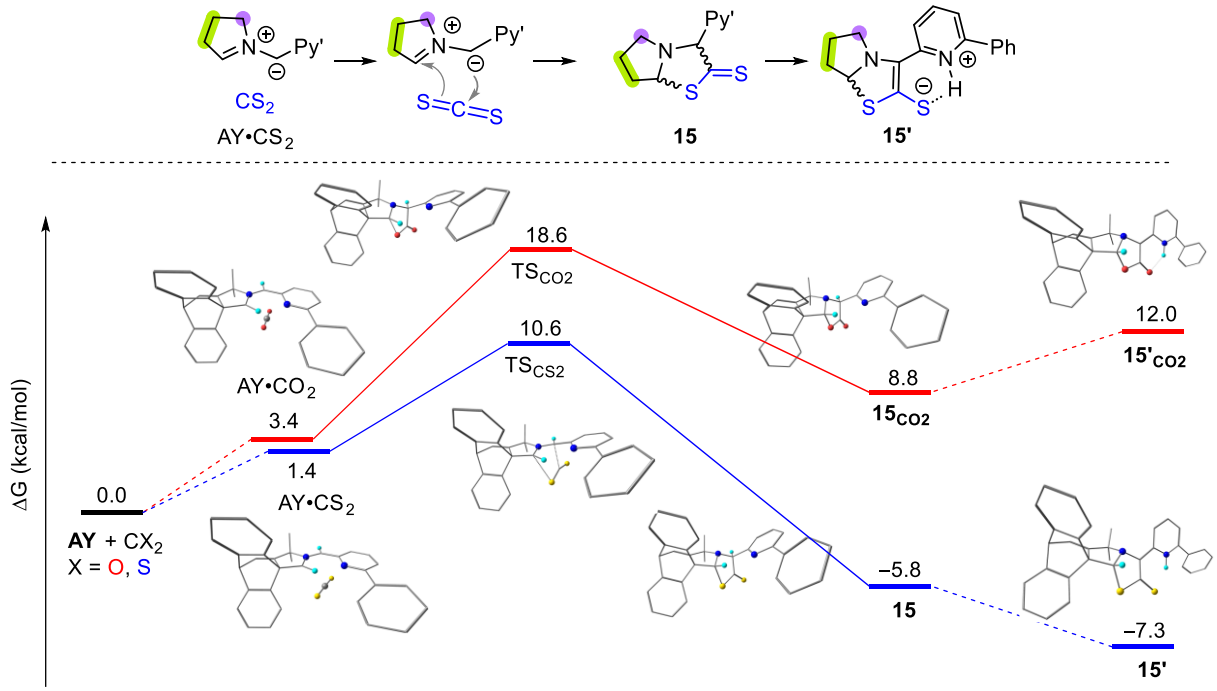

Figure 9. DFT-established mechanism (***top***) for the cycloaddition of CS_2 with **AY** and the corresponding energy profile diagram calculated at B3LYP-D3(BJ)/B2//B3LYP-D3(BJ)/B1 level of theory (***bottom***). The hypothetical CO_2 addition is also included in the same diagram.

DFT analysis performed on a series of P/N-based FLPs shows that ring strain can influence the relative energy barriers for the cycloadditions of CO_2 and CS_2.[13a, 13b, 30] Importantly, from the reactant perspective, the bond dissociation energy of C=S (105.3 kcal/mol) is smaller than C=O (127.2 kcal/mol), which implies that the CS_2 insertion might be easier.[31] But the reversal of polarity of C=S in CS_2 with respect to C=O in CO_2 might lead to electrostatic repulsion of FLPs from CS_2 as opposed to attraction to CO_2.[13a, 13b]

Apart from CS_2, **AY** is shown to undergo 3+2-cycloadditions with a few other dipolarophiles to give a range of N-heterocycles (Scheme 2). For example, dimethyl maleate gives the pyrrolidene **16** which is also confirmed by X-ray crystallography (Figure S72; SI). Like CS_2, dimethyl but-2-ynedioate undergoes cycloaddition followed by tautomerization to give the 2-pyrroline **17**, as indicated by the NMR spectroscopy. Benzophenone and phenyl isocyanate afford the oxazolidines **18** and **19**, respectively. **18** is additionally recognized by X-ray

crystallography (Figure S73; SI). Acetonitrile also follows the sequence of cycloaddition-tautomerization to give the 2-imidazoline **20** as indicated by NMR spectroscopy.

Table 1. Selective list of bond distances and angles associated with the cycloaddition of AY with CS_2 and hypothetically with CO_2.

	$\angle C_{pyrr}$-N-C_{pico}	∠X-C-X	C–X_{endo}	C_{pico}–C	C_{pyrr}–X_{endo}
AY	129.8	-	-	-	-
CO_2	-	180	1.17	-	-
CS_2	-	180	1.56	-	-
AY•CO_2	129.7	177.3	1.17	3.08	3.34
AY•CS_2	129.7	179.1	1.56	3.41	3.42
15_{CO2}	104.2	123.9	1.35	1.54	1.47
15	110.8	126.8	1.73	1.55	1.93
$15'_{CO2}$	101.7	122.2	1.38	1.43	1.47
15'	108.4	120.0	1.78	1.41	1.90

X = O, S; X_{endo} = **X** on the ring.

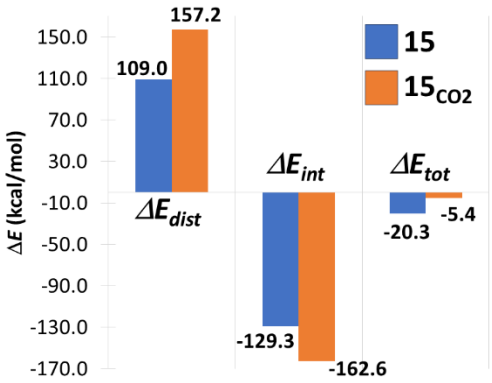

Figure 10. Variations in ΔE_{dis}, ΔE_{int}, ΔE_{tot} between the CO_2 and CS_2 inserted products.

Conclusion

In summary, azomethine ylide, a versatile synthon in organic chemistry, makes a debut as a metal-free intramolecular FLP by unprecedentedly cleaving various E–H (E = B, Si, Al, O) and B–B bonds apart from cycloadding several dipolarophiles. Even in the latter reaction type, the present ylide counter-intuitively favors CS_2 but disfavors a CO_2 insertion. Though the ylide fails to activate H_2, a transfer hydrogenation by NH_3•BH_3 is easily accomplished. The reaction mechanisms including a rationale for the alluring 'CS_2 *vs.* CO_2' selectivity are intensely probed by DFT calculations. Overall, the findings open up newer avenues for both azomethine ylides and FLPs. What is more fascinating is the fact that the activation mechanisms are quite diverse, which advocates a vast range of potential outreach of azomethine ylides as FLPs. This could prove to be a powerful tool for mimicking transition metal chemistry on a purely organic platform. We now focus on designing other azomethine ylides that can be more effective as FLPs and also on implementing this concept into catalytic processes.

Experimental Section

General methods and instrumentation.

All experiments were carried out under dry and oxygen-free nitrogen using standard Schlenk techniques or in an argon-filled glove box (MBraun), unless otherwise mentioned. Prior to use, glassware were dried overnight at 130 °C and solvents were dried, distilled and degassed using standard methods and stored in activated 4 Å molecule sieve in the glove box. **AY**,[9] cyclic imine precursor (**A**)[32] and 2-iodobenzylbromide[33] were prepared following our previously reported literature procedure. All other reagents are available commercially. ^{1}H, ^{13}C{^{1}H}, ^{11}B, ^{19}F and ^{29}Si NMR spectra were recorded either in Bruker spectrometer (Avance NEO or Avance III) operating at 500 MHz or JEOL (JNM ECZL-400S) operating at 400 MHz at ambient temperature. Structural assignments were made with additional information from gCOSY, gHSQC, and gDEPT. experiments. Mass spectrometric analyses were done on a Waters Spectrometer. X-ray diffraction data were collected on either a Rigaku Synergy i xtalab diffractometer or a Bruker D8 diffractometer. All NMR spectra (Figure S1-S70), the summary of crystal data and structural refinements (Table S1-S2), and a summary of computational details are given in their respective sections. The crystallographic data for the structures reported in this article have been deposited at the Cambridge Crystallographic Data Centre, under the deposition numbers 2392878 (**1**), CCDC-2392879 (**9**), CCDC- 2392881 (**11**), CCDC- 2394619 (**14**), CCDC- 2392882 (**15'**), CCDC- 2392883 (**16**), and CCDC-2392884 (**18**). The data can be obtained free of charge via https://www.ccdc.cam.ac.uk/structures/.

1: A 10 mL glass vial fitted with a magnetic bead was charged with **AY** (0.100 g, 0.228 mmol) and dissolved in 1 mL of benzene. Another benzene solution of HBpin (0.031 g, 0.239 mmol) was slowly added into it and the reaction mixture was stirred at room temperature for 1 h, during which the color changed to light yellow. All volatiles were then removed under reduced pressure, and the residue was washed with chilled hexane. Drying the solid under high vacuum gave **1** as a colorless microcrystalline solid (0.107 g, 0.187 mmol, 82%). Colorless X-ray suitable crystals were grown from concentrated hexane solution at low temperatures.

^{1}H NMR (400 MHz, $CDCl_3$) δ 8.06 (d, *J* = 7.0 Hz, 2H, Ar-*H*), 7.74 – 7.64 (m, 2H, Ar-*H*), 7.58 – 7.54 (m, 1H, Ar-*H*), 7.48 – 7.42 (m, 2H, Ar-*H*), 7.42 – 7.33 (m, 2H, Ar-*H*), 7.32 – 7.22 (m, 3H, Ar-*H*), 7.03 – 6.93 (m, 4H, Ar-*H*), 6.47 (d, *J* = 5.8 Hz, 1H, olefinic-C*H*), 5.13 (d, *J* = 5.8 Hz, 1H, olefinic-C*H*), 4.28 (d, *J* = 10.3 Hz, 1H, N-CH_2), 4.21 (d, *J* = 10.3 Hz, 1H, N-CH_2), 4.10 (s, 1H, C*H*B), 1.40 (s, 6H, CH_3), 1.33 (s, 6H, CH_3), 1.09 (s, 6H, CH_3). ^{13}C{^{1}H} NMR (101 MHz, $CDCl_3$) δ 165.2, 165.0, 156.1, 148.1, 148.0, 147.3, 147.0, 140.0, 137.2, 128.7, 128.6, 127.3, 124.4, 124.3, 124.2, 122.9, 122.8, 120.7, 120.2, 119.9, 118.0, 83.9, 61.8, 59.3, 51.6, 46.6, 26.0, 25.3, 25.2, 22.4. ^{11}B NMR (128 MHz, $CDCl_3$) δ 20.03. HRMS-(m/z): [M+H] calc. for [$C_{38}H_{39}BN_2O_2$], 567.3183 found 567.3160.

2[Br]: A 100 mL thick-walled and teflon-capped tube with a J. Young-styled valve on the side was charged with **A** (0.730 g, 2.690 mmol), 2-Iodobenzyl bromide (0.798 g, 2.690 mmol), and 8 mL of CH_3CN. The reaction was then heated to 50 ºC for

48 h under stirring conditions. All volatiles were then removed under reduced pressure to obtain a white residue, which was further washed with Et_2O to afford **2[Br]** (1.187 g, 2.090 mmol, 85%) as a white solid.

^{1}H NMR (400 MHz, $CDCl_3$) δ 11.53 (s, 1H, iminium-C*H*), 7.99 – 7.90 (m, 3H, Ar-*H*), 7.83 (t, *J* = 7.7 Hz, 1H, Ar-*H*), 7.74 (d, *J* = 7.4 Hz, 2H, Ar-*H*), 7.69 – 7.65 (m, 1H, Ar-*H*), 7.52 – 7.47 (m, 3H, Ar-*H*), 7.32 – 7.25 (m, 3H, Ar-*H*), 6.96 (t, *J* = 7.5, 2H, Ar-*H*), 6.84 (d, *J* = 5.9Hz, 1H, olefinic-C*H*), 6.72 (t, *J* = 7.6Hz, 2H, Ar-*H*), 6.49 (s, 2H, benzyl-CH_2), 5.26 (d, *J* = 5.9 Hz, 1H, olefinic-C*H*), 1.50 (s, 6H, CH_3).^{13}C{^{1}H} NMR (101 MHz, DMSO-D_6) δ 178.4, 153.1, 144.1, 143.0, 140.6, 133.9, 132.8, 132.3, 130.7, 129.7, 125.8, 124.7, 124.1, 121.7, 102.2, 79.3, 66.4, 58.6, 50.4, 26.5. HRMS-(m/z): [M+H] calc. for [$C_{27}H_{23}IN^+$], 489.0904 found 489.0913.

3 and **4**: A Screw cap NMR tube was charged with **2[Br]** (0.033 g, 0.058 mmol) and added to it a 0.6 mL C_6D_6 solution of KMHDS (0.012 g, 0.058 mmol). The color changed to light orange immediately after the addition. Recording the ^{1}H NMR spectrum at this stage indicated the formation of **3**. The color slowly turned to light yellow within 6 hours, and recording the ^{1}H NMR spectrum at this stage showed the complete conversion of **3** into **4**. which is monitored by ^{1}H NMR. **4** was also isolated at the end.

3: ^{1}H NMR (400 MHz, C_6D_6) δ 7.88 -7.84 (m, 2H, Ar-*H*), 7.31 -7.29 (m, 1H, Ar-*H*), 7.16 – 7.08 (m, 3H, Ar-*H*), 7.08 – 7.04 (m, 2H,Ar-*H*), 7.01 (s, 1H, NC*H*), 6.84 – 6.74 (m, 4H, Ar-*H*), 6.38 (m, 1H, Ar-*H*), 6.12 (d, *J* = 5.9 Hz, 1H, olefinic-C*H*), 5.89 (s, 1H, NC*H*), 4.75 (d, *J* = 5.8 Hz, 1H, olefinic-C*H*), 1.14 (s, 6H, CH_3), 0.04 (s, 18H, Si(CH_3)$_3$).

4: ^{1}H NMR (400 MHz, C_6D_6) δ 7.66 –7.64 (m, 1H, Ar-*H*), 7.48 – 7.42 (m, 2H, Ar-*H*), 7.25 – 7.20 (m, 1H, Ar-*H*), 7.09 – 7.03 (m, 2H, Ar-*H*), 7.02 – 6.94 (m, 2H, Ar-*H*), 6.89 – 6.87 (m, 1H, Ar-*H*), 6.82 – 6.72 (m, 3H, Ar-*H*), 6.57 – 6.55 (m, 1H, Ar-*H*), 6.10 (d, *J* = 5.9 Hz, 1H, olefinic-C*H*), 4.72 (d, *J* = 5.9 Hz, 1H, olefinic-C*H*), 3.31 (d, *J* = 2.3 Hz, 1H, NC*H*), 3.08 (d, *J* = 2.3 Hz, 1H, NC*H*), 1.13 (d, *J* = 1.9 Hz, 6H, CH_3), 0.03 (s, 18H, Si(CH_3)$_3$).^{13}C{^{1}H} NMR (101 MHz, $CDCl_3$) δ 165.2, 147.8, 146.7, 146.6, 142.2, 139.5, 129.0, 128.8, 127.9, 126.9, 124.9, 124.9, 124.6, 124.4, 123.4, 122.9, 122.6, 119.6, 99.2, 66.7, 65.6, 52.1, 48.4, 48.1, 33.5, 25.4. HRMS-(m/z): [M+H] calc. for [$C_{27}H_{22}IN$], 488.0870 found 488.0879.

5: A screw cap NMR tube was charged with **2[Br]** (0.063 g, 0.110 mmol) followed by adding 0.4 mL C_6D_6 solution of KMHDS (0.022 g, 0.110 mmol) into it. The color changed to a light orange immediately following the addition. After 2 minutes, a 0.2 mL C_6D_6 solution of HBpin (0.014 g, 0.110 mmol) was added to the NMR tube and mixed well for 10 min, during which noticed a decolorization. Recording the NMR spectrum at this stage showed the formation of **5**.

^{1}H NMR (400 MHz, C_6D_6) δ 7.99 (d, *J* = 7.8 Hz, 1H, Ar-*H*), 7.71 – 7.45 (m, 2H, Ar-*H*), 7.27 (d, *J* = 7.4 Hz, 1H, Ar-*H*), 7.07 (d, *J* = 1.9 Hz, 1H, Ar-*H*), 6.99 (t, *J* = 7.5 Hz, 1H, Ar-*H*), 6.93 – 6.70 (m, 5H, Ar-*H*), 6.52 – 6.39 (m, 1H, Ar-*H*), 6.15 (d, *J* = 5.9 Hz, 1H, olefinic-C*H*), 4.81 (d, *J* = 5.9 Hz, 1H, olefinic-C*H*), 4.44 (d, *J* = 9.9 Hz, 1H, NCH_2), 4.32 (s, 1H, BC*H*), 4.28 (d, *J* = 9.9 Hz, 1H, NCH_2), 1.14 (s, 3H, CH_3), 1.03 (d, *J* = 4.4 Hz, 12H, CH_3), 0.80 (s, 3H, CH_3), 0.04 (m, 18H, Si(CH_3)$_3$).^{13}C{^{1}H} NMR (101 MHz, C_6D_6) δ 165.6, 148.6, 147.7, 147.5, 146.8, 139.5, 131.8, 125.0, 124.9, 124.8, 123.5, 123.4, 120.9, 120.4, 99.3, 84.4, 63.1, 59.7, 52.2, 49.7, 26.3, 25.3, 25.3, 22.1, 3.0. ^{11}B NMR (128 MHz, C_6D_6) δ 24.54. HRMS-(m/z): [M+H] calc. for [$C_{33}H_{35}BINO_2$], 616.1884 found 616.1887.

6: A 10 mL glass vial fitted with a magnetic bead was charged with **AY** (0.100 g, 0.228 mmol) and dissolved in 1 mL of benzene. BF_3.Et_2O (0.033 g, 0.228 mmol) was slowly added into it and the reaction mixture was stirred at room temperature for 1 h, during which a white solid was precipitated. The solid was isolated by filtration and washed with hexane (5 × 5 mL). Finally, drying the solid under high vacuum gave **6** as a colorless and air-moisture sensitive solid (0.090 g, 0.177 mmol, 78%).

^{1}H NMR (400 MHz, $CDCl_3$) δ 10.30 (s, 1H, pyr-*H*), 7.88 (m, 2H, Ar-*H*), 7.77 (t, *J* = 7.7 Hz, 1H, Ar-*H*), 7.54 – 7.48 (m, 4H, Ar-*H*), 7.47 – 7.43 (m, 2H, Ar-*H*), 7.38 – 7.35 (m, 1H, Ar-*H*), 7.30 (dd, *J* = 7.4, 1.6 Hz, 1H, Ar-*H*), 7.19 – 7.15 (m, 1H, Ar-*H*), 7.10 – 7.03 (m, 2H, Ar-*H*), 6.91 (m, 1H, Ar-*H*), 6.83 (d, *J* = 5.9 Hz, 1H, olefinic-C*H*), 6.34 (t, *J* = 7.5Hz, 1H, Ar-*H*), 5.29 (d, *J* = 5.9 Hz, 1H, olefinic-C*H*), 4.82 (s, 1H, pico-C*H*), 1.63 (s, 3H, CH_3), 1.22 (s, 3H, CH_3). ^{13}C{^{1}H} NMR (101 MHz, $CDCl_3$) δ 173.2, 157.5, 155.4, 153.7, 143.7, 143.6, 142.6, 140.6, 137.6, 129.7, 126.0, 125.7, 125.7, 125.1, 123.8, 123.6, 121.8, 121.2, 120.2, 119.8, 78.3, 67.0, 51.6, 27.0, 26.3. ^{19}F NMR (376 MHz, $CDCl_3$) δ -149.9. ^{11}B NMR (128 MHz, $CDCl_3$) δ 1.08 (d, *J* = 50.3 Hz). HRMS-(m/z): [M+Na] calc. for [$C_{32}H_{26}BF_3N_2$], 529.2039 found 529.2025.

7: A 10 mL glass vial fitted with a magnetic bead was charged with **AY** (0.100 g, 0.228 mmol) and dissolved in 1 mL of benzene. Another 1 mL benzene solution of $B(C_6F_5)_3$ (0.117 g 0.228 mmol) was slowly added into it and the reaction mixture was stirred at room temperature for 3 h to give a colorless solution. All volatiles were removed under reduced pressure and the residue was washed with hexane (5 × 5 mL) to obtain a colorless solid. Drying the solid under high vacuum gave **7** as a colorless solid (0.174 g, 0.182 mmol, 80%).

^{1}H NMR (400 MHz, C_6D_6) δ 10.12 (s, 1H, pyr-*H*), 7.55 – 7.49 (m, 2H, Ar-*H*), 7.39 – 7.35 (m, 1H, Ar-*H*), 7.24 – 7.04 (m, 7H, Ar-*H*), 6.92 – 6.83 (m, 2H, Ar-*H*), 6.80 (dd, *J* = 7.4, 1.1 Hz, 1H, Ar-*H*), 6.69 (dd, *J* = 7.8, 0.9 Hz, 1H, Ar-*H*), 6.65 – 6.59 (m, 2H), 6.55 (m, 1H, Ar-*H*), 6.36 (m, 1H, Ar-*H*), 5.84 (d, *J* = 6.0, 1H, olefinic-C*H*), 5.80 – 5.74 (m, 1H, pico-C*H*), 4.48 (d, *J* = 6.0 Hz, 1H, olefinic-C*H*), 1.29 (s, 3H, CH_3), 0.20 (s, 3H, CH_3). ^{13}C{^{1}H} NMR (101 MHz, C_6D_6) δ 176.7, 158.9, 157.6, 153.6, 150.3, 148.0, 144.4, 143.8, 143.6, 143.2, 141.1, 139.7, 139.3, 138.6, 138.1, 136.8, 129.7, 129.4, 129.25, 128.9, 127.9, 126.7, 126.2, 125.5, 125.4, 124.4, 124.1, 122.0, 120.6, 119.8, 119.7, 82.3, 67.2, 51.7, 30.5, 26.0. ^{19}F NMR (376 MHz, C_6D_6) δ -127.61 (br, 6F), -158.38 (t, *J* = 21.0 Hz, 3F), -163.75 (br, 6F). ^{11}B NMR (128 MHz, $CDCl_3$) δ -11.66 (s).

8: A 10 mL glass vial fitted with a magnetic bead was charged with **AY** (0.100 g, 0.228 mmol) and dissolved in 1 mL of benzene. Another 1 mL benzene solution of $PhSiH_3$ (0.049 g, 0.456 mmol) was slowly added and the reaction mixture was stirred at room temperature for 10 h, during which the color changed to light yellow. Removing under reduced pressure gave **8** as an oil (0.115 g, 0.209 mmol, 92%).

^{1}H NMR (400 MHz, C_6D_6) δ 8.03 (d, *J* = 7.0 Hz, 2H, Ar-*H*), 7.68 (d, *J* = 4.8 Hz, 2H, Ar-*H*), 7.36 (dd, *J* = 7.0, 1.6 Hz, 1H, Ar-*H*), 7.23 (m, 4H, Ar-*H*), 7.19 – 7.10 (m, 4H, Ar-*H*), 7.05 (d, *J* = 6.3 Hz, 4H, Ar-*H*), 6.81 (m, 4H, Ar-*H*), 6.17 (d, *J* = 5.9 Hz, 1H, olefinic-C*H*), 5.24 (dd, *J* = 6.9, 2.9 Hz, 1H, SiH_2), 5.08 (dd, *J* = 6.9, 2.9 Hz, 1H, SiH_2), 4.80 (d, *J* = 5.8 Hz, 1H, olefinic-

C*H*), 4.54 (d, *J* = 9.8 Hz, 1H,NCH_2), 4.50 – 4.44 (m, 2H, NCH_2 and NC*H*), 0.95 (s, 3H, CH_3), 0.80 (s, 3H, CH_3). $^{13}C\{^1H\}$ NMR (101 MHz, C_6D_6) δ 165.4, 165.1, 156.7, 148.6, 148.4, 147.4, 147.4, 140.2, 137.5, 140.0, 136.5, 133.1, 130.4, 130.3, 129.5, 129.2, 128.9, 127.8, 125.1, 125.0, 124.8, 124.7, 123.5, 123.4, 121.3, 121.1, 120.4, 118.0, 62.9, 56.0, 52.6, 52.2, 47.8, 26.3, 23.2. ^{29}Si NMR (79 MHz, C_6D_6) δ -31.7(t, J_{Si-H} = 173 Hz). HRMS-(m/z): [M+H] calc. for [$C_{38}H_{34}N_2Si$], 547.2570 found 547.2582.

9: A 10 mL glass vial fitted with a magnetic bead was charged with **AY** (0.100 g, 0.228 mmol) and dissolved in 1 mL of benzene. A 0.5 M toluene solution of $AlH_3.N(Me)_2Et$ (456 μL, 0.228 mmol) was added dropwise into it and the reaction mixture was stirred at room temperature for 5 h, during which the color changed to dark red. Removing the volatiles under reduced pressure gave **9** as a dark red solid (0.091 g, 0.193 mmol, 85%). X-ray quality single crystals were grown from a concentrated hexane solution at – 30 °C.

^1H NMR (500 MHz, C_6D_6) δ 7.85 (d, *J* = 7.5 Hz, 2H, Ar-*H*), 7.21 (t, *J* = 7.6 Hz, 2H, Ar-*H*), 7.13 – 6.98 (m, 5H, Ar-*H*), 6.92 – 6.80 (m, 3H, Ar-*H*), 6.76 (t, *J* = 7.4 Hz, 1H, Ar-*H*), 6.70 (t, *J* = 7.6 Hz, 1H, Ar-*H*), 6.22 (dd, *J* = 9.3, 6.3 Hz, 1H, dPy-*H*), 6.07 (d, *J* = 6.0 Hz, 1H, olefinic-C*H*), 5.57 (d, *J* = 9.2 Hz, 1H, dPy-*H*), 5.31 (d, *J* = 6.3 Hz, 1H, dPy-*H*), 4.71 (d, *J* = 6.0 Hz, 1H, olefinic-C*H*), 4.68 (d, *J* = 12.9 Hz, 1H, NCH_2), 4.51 (br, 2H, AlH_2), 4.13 (s, 1H, NC*H*), 4.06 (d, *J* = 12.9 Hz, 1H, NCH_2), 1.16 (s, 3H, CH_3), 1.14 (s, 3H, CH_3). $^{13}C\{^1H\}$ NMR (101 MHz, C_6D_6) δ 161.6, 153.2, 148.5, 147.6, 146.7, 146.5, 146.4, 141.3, 132.4, 129.7, 129.6, 129.4, 128.9, 128.9, 127.3, 126.0, 125.3, 125.2, 125.2, 124.6, 123.4, 123.2, 122.0, 120.4, 113.7, 101.0, 96.8, 69.3, 59.8, 58.0, 52.2, 25.4, 22.2. Elemental analysis for $C_{32}H_{29}N_2Al$: Calculated C 82.02; H 6.24; N 5.98; Found C 81.88; H 6.32; N 5.89.

10-D_2O: A screw cap (fitted with a septum) NMR tube was charged with a C_6H_6 solution of **AY** (0.050 g, 0.114 mmol). Degassed D_2O (0.005 g, 0.249 mmol, 5 μL) was then added into it through a microliter syringe. The NMR tube was sonicated for 10 minutes to obtain a colorless solution. Recording the ^2H NMR spectrum at this stage showed the formation of **10-D_2O**.

^2H NMR (77 MHz, C_6H_6) δ 5.61 (br, 1H), 4.10 (m, 1H).

11: A 10 mL glass vial fitted with a magnetic bead was charged with **AY** (0.100 g, 0.228 mmol) and dissolved in 1 mL of benzene. Another 1 mL benzene solution of $PhCH_2OH$ (0.025 g, 0.228 mmol) was added to it and the reaction mixture was stirred at room temperature for 1 h to obtain a colorless solution. Removing the volatiles under reduced pressure gave **11** as a colorless solid (0.101 g, 0.184 mmol, 81%). X-ray suitable single crystals were grown from its concentrated hexane solution.

^1H NMR (500 MHz, C_6D_6) δ 8.29 (d, *J* = 8.4, 2H, Ar-*H*), 8.22 – 8.15 (m, 1H, Ar-*H*), 7.66 (d, *J* = 7.6, 1H, Ar-*H*), 7.41 – 7.28 (m, 7H, Ar-*H*), 7.26 – 7.17 (m, 2H, Ar-*H*), 7.15 – 7.10 (m, 3H, Ar-*H*), 7.08 – 7.03 (m, 1H, Ar-*H*), 6.93 (m, 1H, Ar-*H*), 6.88 (m, 1H, Ar-*H*), 6.86 – 6.82 (m, 2H, Ar-*H*), 6.35 (d, *J* = 6.0 Hz, 1H, olefinic-C*H*), 5.85 (s, 1H, NC*H*O), 4.97 (d, *J* = 11.4 Hz, 1H, pico-CH_2), 4.86 (d, *J* = 6.0 Hz, 1H, olefinic-C*H*), 4.74 (d, *J* = 11.4 Hz, 1H, pico-CH_2), 4.48 (d, *J* = 15.8 Hz, 1H, OCH_2), 4.12 (d, *J* = 15.7 Hz, 1H, OCH_2), 1.19 (s, 3H, CH_3), 0.95 (s, 3H, CH_3).$^{13}C\{^1H\}$ NMR (101 MHz, C_6D_6) δ 163.9, 162.5, 156.4, 149.0, 148.5, 148.2, 146.3, 140.4, 139.3, 137.3, 129.4, 129.3, 128.9, 127.9, 127.6, 126.2, 125.3, 125.1, 124.9, 124.7, 124.6, 123.5, 123.3, 121.9, 121.1, 118.5, 95.9, 73.2, 62.5, 61.0, 52.7, 51.0, 27.1, 25.6.

12: A 10 mL glass vial fitted with a magnetic bead was charged with **AY** (0.100 g, 0.228 mmol) and dissolved in 1 mL of benzene. Another 1 mL benzene solution of CH_3I (0.033 g, 0.233 mmol) was added to it and the reaction mixture was stirred at room temperature for 12 h, during which a white precipitate appeared. The precipitate was washed with benzene (3 × 5 mL) and dried under vacuum to obtain **12** as a colorless powder (0.125 g, 0.215 mmol, 94%).

^1H NMR (500 MHz, $CDCl_3$) δ 10.93 (s, 1H, pyr-C*H*), 8.45 (d, *J* = 7.7 Hz, 1H, Ar-*H*), 8.03 (d, *J* = 7.5 Hz, 2H, Ar-*H*), 7.90 (t, *J* = 7.6 Hz, 1H, Ar-*H*), 7.72 (d, *J* = 8.0 Hz, 1H, Ar-*H*), 7.58 (dd, *J* = 15.1, 7.4 Hz, 4H, Ar-*H*), 7.38 (d, *J* = 7.9 Hz, 1H, Ar-*H*), 7.25 (br, 1H, Ar-*H*), 7.09 (d, *J* = 5.6 Hz, 2H, Ar-*H*), 7.01 (d, *J* = 7.0 Hz, 1H, Ar-*H*), 6.95 (d, *J* = 7.5 Hz, 1H, Ar-*H*), 6.91 – 6.82 (m, 2H Ar-*H* and olefinic-C*H*), 6.20 (t, *J* = 7.6 Hz, 1H, pico-C*H*), 5.28 (d, *J* = 5.4 Hz, 1H, olefinic-C*H*), 2.32 (d, *J* = 6.9 Hz, 3H, pico-CH-CH_3), 1.93 (s, 3H, CH_3), 1.44 (s, 3H, CH_3). $^{13}C\{^1H\}$ NMR (126 MHz, DMSO-d_6) δ 179.5, 157.9, 154.7, 152.7, 144.5, 144.5, 143.5, 143.5, 140.1, 138.8, 131.2, 130.3, 129.6, 128.1, 126.6, 126.3, 125.6, 124.8, 124.7, 124.6, 122.1, 121.9, 121.6, 121.5, 79.9, 67.3, 60.6, 50.9, 27.0, 26.1, 24.3. HRMS-(m/z): $[M]^+$ calc. for $[C_{33}H_{29}N_2]^+$, 453.2325 found 453.2318.

13: A 50 mL storage flask with a J. Young-type Teflon valve and fitted with a magnetic bead was charged with a benzene solution of **AY** (0.200 g, 0.456 mmol) and B_2Pin_2 (0.116 g, 0.456 mmol). The reaction mixture was stirred at 40 °C for four days, during which the solution turned from deep yellow to faint yellow. Removing the volatiles under reduced pressure gave a light-yellow residue, which was washed with hexane (5 × 5 mL) to obtain a light-yellow solid. Drying the solid under high vacuum gave **13** as a light-yellow powder (0.252 g, 0.364 mmol, 80%).

^1H NMR (500 MHz, -20 °C, Tol-d_8) δ 8.26 (d, *J* = 7.8 Hz, 1H, Ar-*H*), 8.18 (d, *J* = 7.7 Hz, 2H, Ar-*H*), 7.99 (dd, *J* = 42.8, 7.4 Hz, 2H, Ar-*H*), 7.32 (t, *J* = 7.7 Hz, 1H, Ar-*H*), 7.25 – 7.17 (m, 4H, Ar-*H*), 7.14 (d, *J* = 8.2 Hz, 3H, Ar-*H*), 7.04 (d, *J* = 7.6 Hz, 2H, Ar-*H*), 6.76 (t, *J* = 7.4 Hz, 1H, Ar-*H*), 6.27 (d, *J* = 5.9 Hz, 1H, olefinic-C*H*), 5.30 (d, *J* = 15.1 Hz, 1H, pico-CH_2), 4.74 (d, *J* = 5.8 Hz, 1H, olefinic-C*H*), 4.60 (d, *J* = 15.0 Hz, 1H, pico-CH_2), 1.83 (s, 3H, CH_3), 1.31 (s, 6H, CH_3), 1.07 (d, *J* = 19.2 Hz, 18H, CH_3), 0.74 (s, 3H, CH_3).

$^{13}C\{^1H\}$ NMR (126 MHz, –20 °C, Tol-d_8) δ 167.6, 165.2, 154.9, 151.1, 150.2, 145.7, 145.3, 140.1, 136.1, 129.1, 128.5, 128.2, 127.1, 126.9, 126.5, 124.5, 123.4, 123.1, 123.0, 122.8, 122.6, 122.2, 121.1, 117.7, 83.9, 83.6, 65.1, 63.2, 53.6, 52.1, 36.6, 25.5, 25.3, 25.1, 24.9, 24.8, 22.4. ^{11}B NMR (128 MHz, C_6D_6) δ 21.9. HRMS-(m/z): [M+H] calc. for [$C_{44}H_{50}B_2N_2O_4$], 693.4035 found 693.4013.

14: A 10 mL glass vial fitted with a magnetic bead was charged with **AY** (0.100 g, 0.228 mmol) and dissolved in 1 mL of benzene. A 2 mL benzene suspension of NH_3BH_3 (0.008 g, 0.260 mmol) was added to it and the reaction mixture was stirred at room temperature for 10 h, during which the solution color changed to light yellow and a solid was precipitated. The solution was filtered and the volatiles were removed from the filtrate under reduced pressure to obtain **14** as a pale-yellow semi-solid (0.085 g, 0.193 mmol, 85%). X-ray quality single

crystals were grown from a concentrated toluene solution at –40 °C.

^{1}H NMR (400 MHz, C_6D_6): δ 8.33 – 8.21 (m, 2H, Ar-*H*), 7.57 (m, 1H, Ar-*H*), 7.39 – 7.27 (m, 4H, Ar-*H*), 7.21 – 7.14 (m, 1H, Ar-*H*), 7.13 – 7.05 (m, 5H, Ar-*H*), 6.86 – 6.75 (m, 4H, Ar-*H*), 6.21 (d, *J* = 5.9 Hz, 1H, olefinic-C*H*), 4.80 (d, *J* = 5.9 Hz, 1H, olefinic-C*H*), 3.96 (s, 2H, NCH_2), 3.74 (s, 2H, NCH_2), 0.87 (s, 6H, CH_3). ^{13}C{^{1}H} NMR (126 MHz, C_6D_6): δ 165.7, 162.1, 156.9, 148.4, 147.5, 140.5, 137.7, 129.3, 128.7, 127.7, 125.2, 124.8, 124.8, 123.4, 120.9, 120.6, 118.7, 61.6, 59.7, 55.4, 52.2, 49.4, 23.1. HRMS-(m/z): [M+H] calc. for [$C_{32}H_{28}N_2$], 441.2331 found 441.2310.

15': A 10 mL glass vial fitted with a magnetic bead was charged with **AY** (0.100 g, 0.228 mmol) and dissolved in 1 mL of benzene. A 5 mL hexane solution of CS_2 (0.050 mL, 0.228 mmol) was slowly added into it and the reaction mixture was stirred at room temperature for 5 h, during which the color changed to dark red. The volatiles were removed under reduced pressure to obtain **15'** as a red solid (0.107 g, 0.207 mmol, 91%). X-ray quality single crystals were grown from a concentrated toluene solution at –30 °C. The NMR spectral data as listed below suggest the existence of **15'** as **15**.

^{1}H NMR (400 MHz, C_6D_6) δ 8.31 (s, 1H, pico-C*H*), 8.17 – 8.11 (m, 2H, Ar-*H*), 7.39 (t, *J* = 7.2 Hz, 2H, Ar-*H*), 7.29 – 7.16 (m, 6H, Ar-*H*), 7.14 – 7.11 (m, 1H, Ar-*H*), 7.00 (dd, *J* = 7.0, 1.2 Hz, 1H, Ar-*H*), 6.85 – 6.75 (m, 2H, Ar-*H*), 6.65 (m, 1H, Ar-*H*), 6.56 (m, 1H, Ar-*H*), 6.28 (d, *J* = 6.1 Hz, 1H, olefinic-C*H*), 5.35 (s, 1H, pyr-C*H*), 4.76 (d, *J* = 6.0 Hz, 1H, olefinic-C*H*), 1.18 (s, 3H, CH_3), 0.96 (s, 3H, CH_3). ^{13}C{^{1}H} NMR (101 MHz, C_6D_6) δ 246.4, 162.9, 159.2, 158.1, 148.3, 147.6, 146.9, 144.5, 140.1, 137.8, 129.7, 129.4, 128.9, 127.8, 127.0, 125.7, 125.1, 124.9, 124.7, 123.8, 123.6, 123.5, 122.2, 120.2, 120.0, 86.9, 84.8, 65.0, 64.6, 52.4, 30.9, 25.3.

16: A 10 mL glass vial fitted with a magnetic bead was charged with **AY** (0.100 g, 0.228 mmol) and dissolved in 1 mL of benzene. Another 1 mL benzene solution of dimethyl maleate (0.033 g, 0.228 mmol) was slowly added into it and the reaction mixture was stirred at room temperature for 10 h, during which the color changed to light yellow and the solution became turbid. All volatiles were removed under reduced pressure and the residue was washed with chilled hexane (3 × 5 mL). Finally, drying the solid under high vacuum gave **16** as a colorless microcrystalline solid (0.119 g, 0.205 mmol, 90%). X-ray suitable single crystals were grown from a concentrated hexane solution at –30 °C.

^{1}H NMR (500 MHz, $CDCl_3$) δ 8.02 (d, *J* = 7.0 Hz, 2H, Ar-*H*), 7.81 (d, *J* = 7.4 Hz, 1H, Ar-*H*), 7.74 – 7.67 (m, 2H, Ar-*H*), 7.56 (dd, *J* = 7.1, 1.7 Hz, 1H, Ar-*H*), 7.51 – 7.46 (m, 2H, Ar-*H*), 7.44 – 7.40 (m, 1H, Ar-*H*), 7.30 (m, 2H, Ar-*H*), 7.22 (m, 1H, Ar-*H*), 7.09 (m, 1H, Ar-*H*), 7.01 (m, 1H, Ar-*H*), 6.96 – 6.89 (m, 2H, Ar-*H*), 6.55 (d, *J* = 6.1 Hz, 1H, olefinic-C*H*), 6.09 (d, *J* = 9.2 Hz, 1H, pico-C*H*), 5.09 (d, *J* = 6.1 Hz, 1H, olefinic-C*H*), 5.05 (d, *J* = 8.5 Hz, 1H, Pyr-C*H*), 4.48-4.42 (m, 1H, COC*H*), 4.38 (t, *J* = 9.5 Hz, 1H, COC*H*), 3.77 (s, 3H, OCH_3), 3.22 (s, 3H, OCH_3), 1.13 (s, 3H, CH_3), 1.03 (s, 3H, CH_3). ^{13}C{^{1}H} NMR (126 MHz, $CDCl_3$) δ 173.0, 172.0, 166.7, 162.5, 156.3, 148.9, 147.9, 147.0, 146.5, 139.7, 137.3, 129.0, 128.5, 127.2, 125.4, 124.8, 124.6, 124.3, 124.3, 123.5, 122.8, 121.6, 121.5, 120.3, 118.9, 66.8, 65.9, 61.6, 61.4, 56.3, 52.5, 52.3, 51.7, 49.9, 29.9, 26.4. HRMS-(m/z): [M] calc. for [$C_{38}H_{34}N_2O_4$], 582.2519 found 583.2596.

17: A 10 mL glass vial fitted with a magnetic bead was charged with **AY** (0.100 g, 0.228 mmol) and dissolved in 1 mL of benzene. Another 1 mL benzene solution of dimethyl but-2-ynedioate (0.0325 g, 0.228 mmol) was slowly added into it and the reaction mixture was stirred at room temperature for 5 h, during which the color changed to light yellow. All volatiles were removed under reduced pressure and the residue was with chilled hexane (3 × 5 mL). Finally, drying the solid under high vacuum gave **17** as a colorless microcrystalline solid (0.118 g, 0.203 mmol, 89%).

^{1}H NMR (400 MHz, $CDCl_3$) d 8.01 – 7.95 (m, 2H, Ar-*H*), 7.88 (m, 1H, Ar-*H*), 7.85 – 7.76 (m, 2H, Ar-*H*), 7.64 (m, 2H, Ar-*H*), 7.47 – 7.34 (m, 3H, Ar-*H*), 7.31 – 7.23 (m, 2H, Ar-*H*), 7.06 (m, 1H, Ar-*H*), 7.02 – 6.90 (m, 3H, Ar-*H*), 6.53 (d, *J* = 6.1 Hz, 1H, olefinic-C*H*), 6.19 (d, *J* = 6.8 Hz, 1H, NC*H*), 5.71 (d, *J* = 6.8 Hz, 1H, COC*H*), 5.08 (d, *J* = 6.0 Hz, 1H, olefinic-C*H*), 3.79 (s, 3H, OCH_3), 3.63 (s, 3H, OCH_3), 1.15 (s, 3H, CH_3), 1.07 (s, 3H, CH_3). ^{13}C{^{1}H} NMR (126 MHz, $CDCl_3$) δ 167.4, 165.1, 163.5, 161.1, 156.2, 148.3, 148.1, 147.6, 147.3, 146.2, 139.3, 137.8, 131.1, 129.1, 128.9, 128.5, 127.0, 125.9, 124.8, 124.6, 124.4, 124.4, 123.2, 122.7, 122.5, 121.9, 120.5, 119.1, 73.6, 70.0, 64.0, 60.8, 52.8, 52.6, 52.5, 32.5, 24.9.HRMS-(m/z): [M+H] calc. for [$C_{38}H_{32}N_2O_4$], 581.2440 found 581.2448.

18: A 10 mL glass vial fitted with a magnetic bead was charged with **AY** (0.100 g, 0.228 mmol) and dissolved in 1 mL of benzene. Another 1 mL benzene solution of benzophenone (0.042 g, 0.228 mmol) was slowly added into it and the reaction mixture was stirred at room temperature for 10 h, during which the color changed to light yellow. All volatiles were removed under reduced pressure and the residue was with chilled hexane (3 × 5 mL). Finally, drying the solid under high vacuum gave **18** as a colorless solid (0.123 g, 0.198 mmol, 87%). X-ray quality single crystals were grown from a concentrated hexane solution at – 30 °C.

^{1}H NMR (500 MHz, C_6D_6) δ 8.91 – 8.80 (m, 1H, Ar-*H*), 8.55 (t, *J* = 6.5 Hz, 2H, Ar-*H*), 8.23 (t, *J* = 6.3 Hz, 2H, Ar-*H*), 7.71 (m, 3H, Ar-*H*), 7.43 – 7.34 (m, 3H, Ar-*H*), 7.26 (m, 5H, Ar-*H*), 7.15 – 6.98 (m, 5H, Ar-*H*), 6.89 (m, 5H, Ar-*H*), 6.76 (br, 1H, NC*H*O), 6.23 (d, *J* = 5.0 Hz, 1H, olefinic-C*H*), 5.97 (br, 1H, pico-C*H*), 4.87 (d, *J* = 5.1 Hz, 1H, olefinic-C*H*), 1.09 – 0.82 (m, 6H, CH_3). ^{13}C{^{1}H} (126 MHz, C_6D_6) δ 165.2, 162.9, 156.0, 148.8, 147.7, 147.5, 145.8, 143.4, 140.4, 137.5, 132.4, 130.6, 129.5, 129.4, 128.9, 128.9, 127.6, 127.6, 127.3, 126.6, 125.7,125.3, 125.2, 125.1, 125.0, 123.7, 123.6, 121.6, 120.3, 118.8, 97.8, 94.3, 74.7, 64.2, 62.1, 52.8, 30.3, 28.5. HRMS-(m/z): [M+H] calc. for [$C_{45}H_{36}N_2O$], 621.2906 found 621.2945.

19: A 10 mL glass vial fitted with a magnetic bead was charged with **AY** (0.100 g, 0.228 mmol) and dissolved in 1 mL of benzene. Another 1 mL benzene solution of phenyl isocyanate (0.027 g, 0.228 mmol) was slowly added into it and the reaction mixture was stirred at room temperature for 5 h, during which the color changed to light yellow. All volatiles were removed under reduced pressure and the residue was with chilled hexane (3 × 5 mL). Finally, drying the solid under high vacuum gave **19** as a light-yellow sticky solid (0.104 g, 0.186 mmol, 82%).

^{1}H NMR (400 MHz, C_6D_6) δ 8.07 – 8.03 (m, 1H, Ar-*H*), 8.03 – 7.99 (m, 2H, Ar-*H*), 7.71 – 7.64 (m, 3H, Ar-*H*), 7.35 – 7.26 (m, 2H, Ar-*H*), 7.24 (m, 1H, Ar-*H*), 7.16 – 7.05 (m, 6H, Ar-*H*), 6.90 – 6.79 (m, 4H, Ar-*H*), 6.76 (m, 1H), 6.67 (m, 1H, Ar-*H*), 6.53 (m, 1H, Ar-*H*), 6.49 (s, 1H, NC*H*O), 6.16 (d, *J* = 6.0 Hz,

1H, olefinic-C*H*), 5.12 (s, 1H, pico-C*H*), 4.74 (d, *J* = 6.0 Hz, 1H, olefinic-C*H*), 0.92 (s, 3H, CH_3), 0.83 (s, 3H, CH_3).^{13}C{^{1}H} (101 MHz, C_6D_6) δ 171.3, 166.1, 161.0, 157.3, 148.6, 147.9, 147.7, 145.7, 140.0, 138.3, 137.6, 129.6, 129.3, 129.1, 127.9, 127.8, 126.9, 126.2, 125.5, 125.5, 125.3, 124.6, 124.1, 123.9, 123.9, 122.1, 121.1, 119.6, 81.0, 68.9, 63.1, 61.3, 53.5, 31.8, 24.7. HRMS-(m/z): [M+H] calc. for [$C_{39}H_{31}N_3O$], 558.2545 found 558.2565.

20: A 10 mL glass vial fitted with a magnetic bead was charged with **AY** (0.100 g, 0.228 mmol) and dissolved in 1 mL of benzene. CH_3CN (0.019 g, 0.456 mmol) was then added dropwise into it and the reaction mixture was stirred at room temperature for 5 h, during which the color changed to light yellow. All volatiles were removed under reduced pressure and the residue was washed with chilled hexane (3 × 5 mL). Drying the solid under high vacuum gave **20** as an off-white solid (0.093 g, 0.193 mmol, 85%).

^{1}H NMR (400 MHz, $CDCl_3$) δ 8.31 – 8.25 (m, 1H, Ar-*H*), 8.11 – 8.04 (m, 2H, Ar-*H*), 7.80 (dd, *J* = 8.1, 7.4 Hz, 1H, Ar-*H*), 7.70 – 7.66 (m, 2H, Ar-*H*), 7.62 (m, 1H, Ar-*H*), 7.54 – 7.41 (m, 3H, Ar-*H*), 7.34 – 7.24 (m, 2H, Ar-*H*), 7.07 – 6.91 (m, 4H, Ar-*H*), 6.81 (m, 1H, NC*H*CH_3), 6.56 (d, *J* = 6.1 Hz, 1H, olefinic-C*H*), 5.16 (d, *J* = 3.5 Hz, 1H, pico-C*H*), 5.11 (d, *J* = 6.1 Hz, 1H, olefinic-C*H*), 2.35 (d, *J* = 1.9Hz, 3H, NCHCH_3), 1.21 (s, 3H, CH_3), 1.04 (s, 3H, CH_3).^{13}C{^{1}H} (101 MHz, $CDCl_3$) δ 174.4, 165.8, 160.3, 156.7, 147.9, 147.9, 147.5, 146.5, 139.6, 137.9, 129.2, 129.0, 128.6, 127.1, 125.2, 124.8, 124.5, 124.5, 124.3, 124.2, 123.0, 122.8, 120.5, 120.0, 119.1, 93.4, 74.3, 61.7, 61.2, 52.4, 31.1, 25.8, 18.2. HRMS-(m/z): [M+H] calc. for [$C_{34}H_{29}N_3$], 480.2440 found 480.2440.

ASSOCIATED CONTENT

Spectroscopic, crystallographic, and computational data.

AUTHOR INFORMATION

Corresponding Author

* d.mukherjee@iiserkol.ac.in

* dibyendu.chem@presiuniv.ac.in

Funding Sources

SERB (DST), Govt. of India for
SRG/2019/001931
SB/S2/RJN-028/2018
CRG/2021/001950
SRG/2019/001461

Notes

The authors declare no competing financial interests.

ACKNOWLEDGMENT

D. Mukherjee thanks SERB, India for SRG/2019/001931 and SB/S2/RJN-028/2018. D. Mallick also thanks SERB, India for SRG/2019/001461 and DST, India for National Supercomputing Mission (DST/NSM/R&D_HPC_Applications/2021/8) for providing computing resources of 'PARAM Shakti' at IIT Kharagpur and ‘PARAM Brahma’ at IISER Pune. SB thanks UGC, India while SS thanks IISER Kolkata for their fellowships.

REFERENCES

1. Welch, G. C.; San Juan, R. R.; Masuda, J. D.; Stephan, D. W., Reversible, metal-free hydrogen activation. *Science* **2006,** *314*, 1124-6.

2. (a) Stephan, D. W., Frustrated Lewis Pairs: From Concept to Catalysis. *Acc. Chem. Res.* **2015,** *48*, 306-316; (b) Stephan, D. W.; Erker, G., Frustrated Lewis pair chemistry: development and perspectives. *Angew. Chem. Int. Ed.* **2015,** *54*, 6400-41; (c) Kehr, G.; Erker, G., Frustrated Lewis Pair Chemistry: Searching for New Reactions. *Chem. Rec.* **2017,** *17*, 803-815; (d) Paradies, J., From structure to novel reactivity in frustrated Lewis pairs. *Coord. Chem. Rev.* **2019,** *380*, 170-183; (e) Jupp, A. R.; Stephan, D. W., New Directions for Frustrated Lewis Pair Chemistry. *Trends Chem.* **2019,** *1*, 35-48; (f) Wilkins, L. C.; Melen, R. L., Small Molecule Activation with Frustrated Lewis Pairs. In *Encyclopedia of Inorganic and Bioinorganic Chemistry*, pp 1-24; (g) Power, P. P., Main-group elements as transition metals. *Nature* **2010,** *463*, 171-177; (h) Slootweg, J. C.; Jupp, A. R., *Frustrated Lewis Pairs*. Springer International Publishing: 2020.

3. (a) Stephan, D. W.; Erker, G., Frustrated Lewis pair chemistry of carbon, nitrogen and sulfur oxides. *Chem. Sci.* **2014,** *5*, 2625-2641; (b) Stephan, D. W., Frustrated Lewis Pairs. *J. Am. Chem. Soc.* **2015,** *137*, 10018-10032; (c) Scott, D. J.; Fuchter, M. J.; Ashley, A. E., Designing effective ‘frustrated Lewis pair’ hydrogenation catalysts. *Chem. Soc. Rev.* **2017,** *46*, 5689-5700; (d) Fontaine, F.-G.; Courtemanche, M.-A.; Légaré, M.-A.; Rochette, É., Design principles in frustrated Lewis pair catalysis for the functionalization of carbon dioxide and heterocycles. *Coord. Chem. Rev.* **2017,** *334*, 124-135; (e) Fontaine, F.-G.; Rochette, É., Ambiphilic Molecules: From Organometallic Curiosity to Metal-Free Catalysts. *Acc. Chem. Res.* **2018,** *51*, 454-464; (f) Hong, M.; Chen, J.; Chen, E. Y. X., Polymerization of Polar Monomers Mediated by Main-Group Lewis Acid–Base Pairs. *Chem. Rev.* **2018,** *118*, 10551-10616; (g) Lam, J.; Szkop, K. M.; Mosaferi, E.; Stephan, D. W., FLP catalysis: main group hydrogenations of organic unsaturated substrates. *Chem. Soc. Rev.* **2019,** *48*, 3592-3612; (h) Stephan, D. W., Diverse Uses of the Reaction of Frustrated Lewis Pair (FLP) with Hydrogen. *J. Am. Chem. Soc.* **2021,** *143*, 20002-20014; (i) Guerzoni, M. G.; Dasgupta, A.; Richards, E.; Melen, R. L., Enantioselective applications of frustrated Lewis pairs in organic synthesis. *Chem Catal.* **2022,** *2*, 2865-2875; (j) Stephan, D. W., Frustrated Lewis pair chemistry of CO. *Chem. Soc. Rev.* **2023,** *52*, 4632-4643; (k) Stefkova, K.; Carden, J. L.; Melen, R. L., 1.06 - Frustrated lewis pairs in catalysis. In *Comprehensive Inorganic Chemistry III (Third Edition)*, Reedijk, J.; Poeppelmeier, K. R., Eds. Elsevier: Oxford, 2023; pp 315-377; (l) Perez-Jimenez, M.; Corona, H.; de la Cruz-Martinez, F.; Campos, J., Donor-Acceptor Activation of Carbon Dioxide. *Chem. Eur. J.* **2023,** *29*, e202301428; (m) Paradies, J., Structure–Reactivity Relationships in Borane-Based FLP-Catalyzed Hydrogenations, Dehydrogenations, and Cycloisomerizations. *Acc. Chem. Res.* **2023,** *56*, 821-834; (n) Khan, M. N.; van Ingen, Y.; Boruah, T.; McLauchlan, A.; Wirth, T.; Melen, R. L., Advances in CO2 activation by frustrated Lewis pairs: from stoichiometric to catalytic reactions. *Chem. Sci.* **2023,** *14*, 13661-13695; (o) Feng, X.; Meng, W.; Du, H., Asymmetric catalysis with FLPs. *Chem. Soc. Rev.* **2023,** *52*, 8580-8598.

4. (a) Guo, Y.; Li, S., Unusual Concerted Lewis Acid−Lewis Base Mechanism for Hydrogen Activation by a Phosphine−Borane Compound. *Inorg. Chem.* **2008,** *47*, 6212-6219; (b) Rokob, T. A.; Hamza, A.; Stirling, A.; Soós, T.; Pápai, I., Turning frustration into bond activation:: a theoretical mechanistic study on heterolytic hydrogen splitting by frustrated Lewis pairs. *Angew Chem Int Ed.* **2008,** *47*, 2435-2438; (c) Stirling, A.; Hamza, A.; Rokob, T. A.; Pápai, I., Concerted attack of frustrated Lewis acid–base pairs on olefinic double bonds: a theoretical study. *Chem. Commun.* **2008**, 3148-3150; (d) Nyhlén, J.; Privalov, T., “Frustration” of Orbital Interactions in Lewis Base/Lewis Acid Adducts: A Computational Study of H2 Uptake by Phosphanylboranes R2P=BR′2. *Eur. J. Inorg. Chem.* **2009,** *2009*, 2759-2764; (e) Rokob, T. A.; Hamza, A.; Pápai, I., Rationalizing the Reactivity of Frustrated Lewis Pairs: Thermodynamics of H2 Activation and the Role of Acid−Base Properties. *J. Am. Chem. Soc.* **2009,** *131*, 10701-10710; (f) Jiang, B.; Zhang, Q.; Dang, L., Theoretical studies on bridged frustrated Lewis pair (FLP) mediated H2 activation and CO2 hydrogenation. *Org. Chem. Front.* **2018,** *5*, 1905-1915; (g) Rokob, T. A.; Bakó, I.; Stirling, A.; Hamza, A.; Pápai, I., Reactivity Models of Hydrogen Activation by Frustrated Lewis Pairs: Synergistic Electron Transfers or Polarization by Electric Field? *J. Am. Chem. Soc.* **2013,** *135*, 4425-4437; (h) Paradies, J., Mechanisms in Frustrated

Lewis Pair-Catalyzed Reactions. *Eur. J. Org. Chem.* **2019,** *2019*, 283-294; (i) Jupp, A. R., Evidence for the encounter complex in frustrated Lewis pair chemistry. *Dalton Trans.* **2022,** *51*, 10681-10689; (j) Zeng, J.; Qiu, R.; Zhu, J., Screening Carbon-Boron Frustrated Lewis Pairs for Small-Molecule Activation including N(2) , O(2) , CO, CO(2) , CS(2) , H(2) O and CH(4) : A Computational Study. *Chem. Asian J.* **2023,** *18*, e202201236; (k) Liu, W. C.; Gabbai, F. P., Characterization of a Lewis adduct in its inner and outer forms. *Science* **2024,** *385*, 1184-1188.

5. Johnstone, T. C.; Wee, G.; Stephan, D. W., Accessing Frustrated Lewis Pair Chemistry from a Spectroscopically Stable and Classical Lewis Acid-Base Adduct. *Angew. Chem. Int. Ed.* **2018,** *57*, 5881-5884.

6. (a) Caputo, C. B.; Stephan, D. W., Non-conventional Lewis Acids and Bases in Frustrated Lewis Pair Chemistry. In *The Chemical Bond III: 100 years old and getting stronger*, Mingos, D. M. P., Ed. Springer International Publishing: Cham, 2017; pp 1-29; (b) Weicker, S. A.; Stephan, D. W., Main Group Lewis Acids in Frustrated Lewis Pair Chemistry: Beyond Electrophilic Boranes. *Bull. Chem. Soc. Jpn.* **2015,** *88*, 1003-1016.

7. (a) Sole, S.; Gornitzka, H.; Schoeller, W. W.; Bourissou, D.; Bertrand, G., (Amino)(aryl)carbenes: stable singlet carbenes featuring a spectator substituent. *Science* **2001,** *292*, 1901-3; (b) Lavallo, V.; Mafhouz, J.; Canac, Y.; Donnadieu, B.; Schoeller, W. W.; Bertrand, G., Synthesis, Reactivity, and Ligand Properties of a Stable Alkyl Carbene. *J. Am. Chem. Soc.* **2004,** *126*, 8670-8671; (c) Lavallo, V.; Canac, Y.; DeHope, A.; Donnadieu, B.; Bertrand, G., A rigid cyclic (alkyl)(amino)carbene ligand leads to isolation of low-coordinate transition-metal complexes. *Angew. Chem. Int. Ed.* **2005,** *44*, 7236-9; (d) Vignolle, J.; Cattoën, X.; Bourissou, D., Stable Noncyclic Singlet Carbenes. *Chem. Rev.* **2009,** *109*, 3333-3384; (e) Melaimi, M.; Soleilhavoup, M.; Bertrand, G., Stable cyclic carbenes and related species beyond diaminocarbenes. *Angew. Chem. Int. Ed.* **2010,** *49*, 8810-49; (f) Martin, D.; Soleilhavoup, M.; Bertrand, G., Stable singlet carbenes as mimics for transition metal centers. *Chem. Sci.* **2011,** *2*, 389-399; (g) Rao, B.; Tang, H.; Zeng, X.; Liu, L. L.; Melaimi, M.; Bertrand, G., Cyclic (Amino)(aryl)carbenes (CAArCs) as Strong sigma-Donating and pi-Accepting Ligands for Transition Metals. *Angew. Chem. Int. Ed.* **2015,** *54*, 14915-9; (h) Soleilhavoup, M.; Bertrand, G., Cyclic (Alkyl)(Amino)Carbenes (CAACs): Stable Carbenes on the Rise. *Acc. Chem. Res.* **2015,** *48*, 256-266; (i) Tomás-Mendivil, E.; Hansmann, M. M.; Weinstein, C. M.; Jazzar, R.; Melaimi, M.; Bertrand, G., Bicyclic (Alkyl)(amino)carbenes (BICAACs): Stable Carbenes More Ambiphilic than CAACs. *J. Am. Chem. Soc.* **2017,** *139*, 7753-7756; (j) Weinstein, C. M.; Junor, G. P.; Tolentino, D. R.; Jazzar, R.; Melaimi, M.; Bertrand, G., Highly Ambiphilic Room Temperature Stable Six-Membered Cyclic (Alkyl)(amino)carbenes. *J. Am. Chem. Soc.* **2018,** *140*, 9255-9260; (k) Loh, Y. K.; Melaimi, M.; Munz, D.; Bertrand, G., An Air-Stable "Masked" Bis(imino)carbene: A Carbon-Based Dual Ambiphile. *J. Am. Chem. Soc.* **2023,** *145*, 2064-2069.

8. (a) Frey, G. D.; Lavallo, V.; Donnadieu, B.; Schoeller, W. W.; Bertrand, G., Facile splitting of hydrogen and ammonia by nucleophilic activation at a single carbon center. *Science* **2007,** *316*, 439-41; (b) Back, O.; Kuchenbeiser, G.; Donnadieu, B.; Bertrand, G., Nonmetal-mediated fragmentation of P4: isolation of P1 and P2 bis(carbene) adducts. *Angew. Chem. Int. Ed.* **2009,** *48*, 5530-3; (c) Frey, G. D.; Masuda, J. D.; Donnadieu, B.; Bertrand, G., Activation of Si-H, B-H, and P-H bonds at a single nonmetal center. *Angew. Chem. Int. Ed.* **2010,** *49*, 9444-7; (d) Dahcheh, F.; Stephan, D. W.; Bertrand, G., Oxidative addition at a carbene center: synthesis of an iminoboryl-CAAC adduct. *Chem. Eur. J.* **2015,** *21*, 199-204; (e) Song, H.; Kim, Y.; Park, J.; Kim, K.; Lee, E., Activation of Small Molecules at N-Heterocyclic Carbene Centers. *Synlett* **2016,** *27*, 477-485; (f) Eichhorn, A. F.; Fuchs, S.; Flock, M.; Marder, T. B.; Radius, U., Reversible Oxidative Addition at Carbon. *Angew. Chem. Int. Ed.* **2017,** *56*, 10209-10213; (g) Eichhorn, A. F.; Kuehn, L.; Marder, T. B.; Radius, U., Facile insertion of a cyclic alkyl(amino) carbene carbon into the B–B bond of diboron(4) reagents. *Chem. Commun.* **2017,** *53*, 11694-11696; (h) Tolentino, D. R.; Neale, S. E.; Isaac, C. J.; Macgregor, S. A.; Whittlesey, M. K.; Jazzar, R.; Bertrand, G., Reductive Elimination at Carbon under Steric Control. *J. Am. Chem. Soc.* **2019,** *141*, 9823-9826; (i) Peltier, J. L.; Tomás-Mendivil, E.; Tolentino, D. R.; Hansmann, M. M.; Jazzar, R.; Bertrand, G., Realizing Metal-Free Carbene-Catalyzed Carbonylation Reactions with CO. *J. Am. Chem. Soc.* **2020,** *142*, 18336-18340.

9. Baguli, S.; Sarkar, S.; Nath, S.; Mallick, D.; Mukherjee, D., Divergent Synthesis of Chelating Aziridines and Cyclic(Alkyl)(Amino)Carbenes (CAACs) from Pyridyl-Tethered Robust Azomethine Ylides. *Angew. Chem. Int. Ed.* **2023,** *62*, e202312858.

10. (a) Coldham, I.; Hufton, R., Intramolecular Dipolar Cycloaddition Reactions of Azomethine Ylides. *Chem. Rev.* **2005,** *105*, 2765-2810; (b) Adrio, J.; Carretero, J. C., Recent advances in the catalytic asymmetric 1,3-dipolar cycloaddition of azomethine ylides. *Chem. Commun.* **2014,** *50*, 12434-12446; (c) Arrastia, I.; Arrieta, A.; Cossio, F. P., Application of 1,3-Dipolar Reactions between Azomethine Ylides and Alkenes to the Synthesis of Catalysts and Biologically Active Compounds. *Eur. J. Org. Chem.* **2018,** *2018*, 5889-5904; (d) Harwood, L. M.; Vickers, R. J., Azomethine Ylides. In *Synthetic Applications of 1,3-Dipolar Cycloaddition Chemistry Toward Heterocycles and Natural Products*, 2002; pp 169-252; (e) Najera, C.; Sansano, M. J., Azomethine Ylides in Organic Synthesis. *Curr. Org. Chem.* **2003,** *7*, 1105-1150; (f) Pandey, G.; Dey, D.; Tiwari, S. K., Synthesis of biologically active natural products by [3+2] cycloaddition of non-stabilized azomethine ylides (AMY): Concepts and realizations. *Tetrahedron Lett.* **2017,** *58*, 699-705.

11. (a) Lopez-Calle, E.; Keller, M.; Eberbach, W., Access to isolable azomethine ylides by photochemical transformation of 2,3-dihydroisoxazoles. *Eur. J. Org. Chem.* **2003,** *2003*, 1438-1453; (b) Song, G.; Chen, D.; Su, Y.; Han, K.; Pan, C. L.; Jia, A.; Li, X., Isolation of azomethine ylides and their complexes: iridium(III)-mediated cyclization of nitrone substrates containing alkynes. *Angew. Chem. Int. Ed.* **2011,** *50*, 7791-6; (c) Lee, D. J.; Han, H. S.; Shin, J.; Yoo, E. J., Multicomponent [5 + 2] Cycloaddition Reaction for the Synthesis of 1,4-Diazepines: Isolation and Reactivity of Azomethine Ylides. *J. Am. Chem. Soc.* **2014,** *136*, 11606-11609; (d) Katayama, K.; Konishi, A.; Horii, K.; Yasuda, M.; Kitamura, C.; Nishida, J.-i.; Kawase, T., Isolation and characterisation of a stable 2-azaphenalenyl azomethine ylide. *Commun. Chem.* **2019,** *2*, 136.

12. (a) Ashley, A. E.; O'Hare, D., FLP-Mediated Activations and Reductions of CO2 and CO. In *Frustrated Lewis Pairs II: Expanding the Scope*, Erker, G.; Stephan, D. W., Eds. Springer Berlin Heidelberg: Berlin, Heidelberg, 2013; pp 191-217; (b) Pal, R.; Ghara, M.; Chattaraj, P. K., Activation of Small Molecules and Hydrogenation of CO Catalyzed by Frustrated Lewis Pairs. *Catalysts* **2022,** *12*, 201; (c) Horton, T. A. R.; Wang, M.; Shaver, M. P., Polymeric frustrated Lewis pairs in CO2/cyclic ether coupling catalysis. *Chem. Sci.* **2022,** *13*, 3845-3850; (d) von Wolff, N.; Lefèvre, G.; Berthet, J. C.; Thuéry, P.; Cantat, T., Implications of CO2 Activation by Frustrated Lewis Pairs in the Catalytic Hydroboration of CO2: A View Using N/Si+ Frustrated Lewis Pairs. *ACS Catal.* **2016,** *6*, 4526-4535; (e) Tran, N.; Ta, Q. T. H.; Nguyen, P. K. T., Transformation of carbon dioxide, a greenhouse gas, into useful components and reducing global warming: A comprehensive review. *Int. J. Energy Res.* **2022,** *46*, 17926-17951.

13. (a) An, K.; Zhu, J., Why Does Activation of the Weaker C═S Bond in CS2 by P/N-Based Frustrated Lewis Pairs Require More Energy Than That of the C═O Bond in CO2? A DFT Study. *Organometallics* **2014,** *33*, 7141-7146; (b) Li, Y.; Zhuang, D.; Qiu, R.; Zhu, J., Aromaticity-promoted CS2 activation by heterocycle-bridged P/N-FLPs: a comparative DFT study with CO2 capture. *Phys. Chem. Chem. Phys.* **2022,** *24*, 2521-2526; (c) Devillard, M.; Declercq, R.; Nicolas, E.; Ehlers, A. W.; Backs, J.; Saffon-Merceron, N.; Bouhadir, G.; Slootweg, J. C.; Uhl, W.; Bourissou, D., A Significant but Constrained Geometry Pt→Al Interaction: Fixation of CO2 and CS2, Activation of H2 and PhCONH2. *J. Am. Chem. Soc.* **2016,** *138*, 4917-4926; (d) Samigullin, K.; Georg, I.; Bolte, M.; Lerner, H. W.; Wagner, M., A Highly Reactive Geminal P/B Frustrated Lewis Pair: Expanding the Scope to C-X (X=Cl, Br) Bond Activation. *Chem. Eur. J.* **2016,** *22*, 3478-3484; (e) Yang, M.-C.; Zhang, Z.-F.; Su, M.-D., Understanding the Reactivity of Combination Reactions of Intramolecular Geminal Group 13 Element/Phosphorus and Gallium/Group 15 Element Frustrated Lewis Pairs with CS2. *Inorg. Chem.* **2022,** *61*, 12959-12976; (f) Szynkiewicz, N.; Ponikiewski, Ł.; Grubba, R., Diphosphination of CO2 and CS2 mediated by frustrated Lewis pairs – catalytic route to

phosphanyl derivatives of formic and dithioformic acid. *Chem. Commun.* **2019,** *55*, 2928-2931; (g) Balueva, A. S.; Nikonov, G. N.; Vul'fson, S. G.; Sarvarova, N. N.; Arbuzov, B. A., Reaction of 1-boryl-2-phosphinoethenes with carbon disulfide. *Bull. Acad. Sci. USSR, Div. Chem. Sci.* **1990,** *39*, 2367-2370; (h) Kroner, J.; Nöth, H.; Polborn, K.; Stolpmann, H.; Tacke, M.; Thomann, M., Beiträge zur Chemie des Bors, 219. (Di-tert-butylphosphanylimino)(2,2,6,6-tetramethylpiperidino)boran: ein BNP-1,3-"Dipol". *Chem. Ber.* **2006,** *126*, 1995-2002.

14. Eisenberger, P.; Bailey, A. M.; Crudden, C. M., Taking the F out of FLP: Simple Lewis Acid–Base Pairs for Mild Reductions with Neutral Boranes via Borenium Ion Catalysis. *J. Am. Chem. Soc.* **2012,** *134*, 17384-17387.

15. (a) Monot, J.; Fensterbank, L.; Malacria, M.; Lacôte, E.; Geib, S. J.; Curran, D. P., CAAC Boranes. Synthesis and characterization of cyclic (alkyl) (amino) carbene borane complexes from BF3 and BH3. *Beilstein J. Org. Chem.* **2010,** *6*, 709-712; (b) Costa, P.; Mieres-Perez, J.; Özkan, N.; Sander, W., Activation of the B−F Bond by Diphenylcarbene: A Reversible 1,2-Fluorine Migration between Boron and Carbon. *Angew. Chem. Int. Ed.* **2017,** *56*, 1760-1764; (c) Döring, S.; Erker, G.; Fröhlich, R.; Meyer, O.; Bergander, K., Reaction of the Lewis Acid Tris(pentafluorophenyl)borane with a Phosphorus Ylide: Competition between Adduct Formation and Electrophilic and Nucleophilic Aromatic Substitution Pathways. *Organometallics* **1998,** *17*, 2183-2187.

16. Mohapatra, C.; Samuel, P. P.; Li, B.; Niepötter, B.; Schürmann, C. J.; Herbst-Irmer, R.; Stalke, D.; Maity, B.; Koley, D.; Roesky, H. W., Insertion of Cyclic Alkyl(amino) Carbene into the Si–H Bonds of Hydrochlorosilanes. *Inorg. Chem.* **2016,** *55*, 1953-1955.

17. Nie, W.; Klare, H. F. T.; Oestreich, M.; Fröhlich, R.; Kehr, G.; Erker, G., Reversible Heterolytic Si–H Bond Activation by an Intramolecular Frustrated Lewis Pair. *Z. Naturforsch., B: J. Chem. Sci.* **2012,** *67*, 987-994.

18. Mandal, C.; Sarkar, S.; Panda, S.; Mallick, D.; Mukherjee, D., Synthesis and reactivity of a heteroleptic magnesium hydride on a dearomatized picolyl-based NNN-chelator. *Dalton Trans.* **2024**, *53*, 17343-17350.

19. Cao, L. L.; Stephan, D. W., Reversible 1,1-hydroaluminations and C–H activation in reactions of a cyclic (alkyl)(amino) carbene with alane. *Chem. Commun.* **2018,** *54*, 8407-8410.

20. Kramer, F., Aluminum in Frustrated Lewis Pair Chemistry. *Angew. Chem. Int. Ed.* **2024,** *63*, e202405207.

21. (a) Roesler, R.; Piers, W. E.; Parvez, M., Synthesis, structural characterization and reactivity of the amino borane 1-(NPh2)-2-[B(C6F5)2]C6H4. *J. Organomet. Chem.* **2003,** *680*, 218-222; (b) Klahn, M.; Spannenberg, A.; Rosenthal, U., Tri-tert-butylphosphonium hydroxytris(pentafluorophenyl)borate. *Acta Crystallogr., Sect. E: Crystallogr. Commun.* **2012,** *68*, o1549; (c) Mo, Z.; Szilvasi, T.; Zhou, Y. P.; Yao, S.; Driess, M., An Intramolecular Silylene Borane Capable of Facile Activation of Small Molecules, Including Metal-Free Dehydrogenation of Water. *Angew. Chem. Int. Ed.* **2017,** *56*, 3699-3702; (d) Sinha, S.; Giri, S., Unraveling H2O activation by intermolecular frustrated Lewis pair. *Chem. Phys. Lett.* **2022,** *799*, 139634; (e) Scott, D. J.; Simmons, T. R.; Lawrence, E. J.; Wildgoose, G. G.; Fuchter, M. J.; Ashley, A. E., Facile Protocol for Water-Tolerant "Frustrated Lewis Pair"-Catalyzed Hydrogenation. *ACS Catal.* **2015,** *5*, 5540-5544; (f) Fasano, V.; Ingleson, M. J., Recent Advances in Water-Tolerance in Frustrated Lewis Pair Chemistry. *Synthesis* **2018,** *50*, 1783-1795; (g) Ou, J.; Zhao, T.; Xiong, W.; Liang, H.; Liu, Q.; Hu, X., Water-resistant FLPs-polymer as recyclable catalysts for selective hydrogenation of alkynes. *Chem. Eng. J.* **2023,** *477*, 147248.

22. Das, A.; Elvers, B. J.; Nayak, M. K.; Chrysochos, N.; Anga, S.; Kumar, A.; Rao, D. K.; Narayanan, T. N.; Schulzke, C.; Yildiz, C. B.; Jana, A., Realizing 1,1-Dehydration of Secondary Alcohols to Carbenes: Pyrrolidin-2-ols as a Source of Cyclic (Alkyl)(Amino)Carbenes. *Angew. Chem. Int. Ed.* **2022,** *61*, e202202637.

23. Gómez, S.; Guerra, D.; López, J. G.; Toro-Labbé, A.; Restrepo, A., A Detailed Look at the Reaction Mechanisms of Substituted Carbenes with Water. *J. Phys. Chem. A* **2013,** *117*, 1991-1999.

24. Vasko, P.; Fuentes, M. Á.; Hicks, J.; Aldridge, S., Reversible O–H bond activation by an intramolecular frustrated Lewis pair. *Dalton Trans.* **2019,** *48*, 2896-2899.

25. (a) Stephens, F. H.; Pons, V.; Tom Baker, R., Ammonia–borane: the hydrogen source par excellence? *Dalton Trans.* **2007**, 2613-2626; (b) Zhao, W.; Li, H.; Zhang, H.; Yang, S.; Riisager, A., Ammonia borane-enabled hydrogen transfer processes: Insights into catalytic strategies and mechanisms. *Green Energy Environ.* **2023,** *8*, 948-971; (c) Faverio, C.; Boselli, M. F.; Medici, F.; Benaglia, M., Ammonia borane as a reducing agent in organic synthesis. *Org. Biomol. Chem.* **2020,** *18*, 7789-7813.

26. (a) Zimmerman, P. M.; Paul, A.; Zhang, Z.; Musgrave, C. B., The Role of Free N-Heterocyclic Carbene (NHC) in the Catalytic Dehydrogenation of Ammonia–Borane in the Nickel NHC System. *Angew. Chem. Int. Ed.* **2009,** *48*, 2201-2205; (b) Miller, A. J. M.; Bercaw, J. E., Dehydrogenation of amine–boranes with a frustrated Lewis pair. *Chem. Commun.* **2010,** *46*, 1709-1711; (c) Sabourin, K. J.; Malcolm, A. C.; McDonald, R.; Ferguson, M. J.; Rivard, E., Metal-free dehydrogenation of amine–boranes by an N-heterocyclic carbene. *Dalton Trans.* **2013,** *42*, 4625-4632; (d) Mo, Z.; Rit, A.; Campos, J.; Kolychev, E. L.; Aldridge, S., Catalytic B–N Dehydrogenation Using Frustrated Lewis Pairs: Evidence for a Chain-Growth Coupling Mechanism. *J. Am. Chem. Soc.* **2016,** *138*, 3306-3309; (e) Boom, D. H. A.; Jupp, A. R.; Slootweg, J. C., Dehydrogenation of Amine-Boranes Using p-Block Compounds. *Chem. Eur. J.* **2019,** *25*, 9133-9152; (f) Oldroyd, N. L.; Chitnis, S. S.; LaPierre, E. A.; Annibale, V. T.; Walsgrove, H. T. G.; Gates, D. P.; Manners, I., Ambient Temperature Carbene-Mediated Depolymerization: Stoichiometric and Catalytic Reactions of N-Heterocyclic- and Cyclic(Alkyl)Amino Carbenes with Poly(N-Methylaminoborane) [MeNH–BH2]n. *J. Am. Chem. Soc.* **2022,** *144*, 23179-23190.

27. (a) Kuchenbeiser, G.; Soleilhavoup, M.; Donnadieu, B.; Bertrand, G., Reactivity of Cyclic (Alkyl)(amino)carbenes (CAACs) and Bis(amino)cyclopropenylidenes (BACs) with Heteroallenes: Comparisons with their N-Heterocyclic Carbene (NHCs) Counterparts. *Chem. Asian J.* **2009,** *4*, 1745-1750; (b) Touj, N.; Mazars, F.; Zaragoza, G.; Delaude, L., Aldiminium and 1,2,3-triazolium dithiocarboxylate zwitterions derived from cyclic (alkyl)(amino) and mesoionic carbenes. *Beilstein J. Org. Chem.* **2023,** *19*, 1947-1956; (c) Delaude, L., Betaine Adducts of N-Heterocyclic Carbenes: Synthesis, Properties, and Reactivity. *Eur. J. Inorg. Chem.* **2009,** *2009*, 1681-1699; (d) Duong, H. A.; Tekavec, T. N.; Arif, A. M.; Louie, J., Reversible carboxylation of N-heterocyclic carbenes. *Chem. Commun.* **2004**, 112-113.

28. Li, Z.; Mayer, R. J.; Ofial, A. R.; Mayr, H., From Carbodiimides to Carbon Dioxide: Quantification of the Electrophilic Reactivities of Heteroallenes. *J. Am. Chem. Soc.* **2020,** *142*, 8383-8402.

29. Ess, D. H.; Houk, K. N., Distortion/Interaction Energy Control of 1,3-Dipolar Cycloaddition Reactivity. *J. Am. Chem. Soc.* **2007,** *129*, 10646-10647.

30. Zhu, J.; An, K., Mechanistic insight into the CO2 capture by amidophosphoranes: interplay of the ring strain and the trans influence determines the reactivity of the frustrated Lewis pairs. *Chem. Asian J.* **2013,** *8*, 3147-51.

31. Luo, Y.-R. Comprehensive Handbook of Chemical Bond Energies; CRC Press: Boca Raton, FL, 2007.

32. Serrato, M. R.; Melaimi, M.; Bertrand, G., Cyclic (amino)(barrelene)carbenes: an original family of CAACs through a novel synthetic pathway. *Chem. Commun.* **2022,** *58*, 7519-7521.

33. Landge, K. P.; Jang, K. S.; Lee, S. Y.; Chi, D. Y., Approach to the Synthesis of Indoline Derivatives from Diaryliodonium Salts. *The J. Org. Chem.* **2012,** *77*, 5705-5713.